Check for updates

N,2,6-Trisubstituted 1H-benzimidazole derivatives as a new scaffold of antimicrobial and anticancer agents: design, synthesis, in vitro evaluation, and in silico studies†

Em Canh Pham, [iD] *a Tuong Vi Le Thi,bh Huong Ha Ly Hong,c Bich Ngoc Vo Thi,c Long B. Vong,*de Thao Thanh Vu,f Duy Duc Vo,g Ngoc Vi Tran Nguyen,h Khanh Nguyen Bao Le*h and Tuyen Ngoc Truong [iD] *h

Compounds containing benzimidazole moiety occupy privileged chemical space for discovering new bioactive substances. In continuation of our recent work, 69 benzimidazole derivatives were designed and synthesized with good to excellent yields of 46–99% using efficient synthesis protocol *i.e.* sodium metabisulfite catalyzed condensation of aromatic aldehydes with *o*-phenylenediamines to form 2-arylbenzimidazole derivatives followed by *N*-alkylation by conventional heating or microwave irradiation for diversification. Potent antibacterial compounds against MSSA and MRSA were discovered such as benzimidazole compounds **3k** (2-(4-nitrophenyl), *N*-benzyl), **3l** (2-(4-chlorophenyl), *N*-(4-chlorobenzyl)), **4c** (2-(4-chlorophenyl), 6-methyl, *N*-benzyl), **4g** (2-(4-nitrophenyl), 6-methyl, *N*-benzyl), and **4j** (2-(4-nitrophenyl), 6-methyl, *N*-(4-chlorobenzyl)) with MIC of 4–16 μg mL^{-1}. In addition, compound **4c** showed good antimicrobial activities (MIC = 16 μg mL^{-1}) against the bacteria strains *Escherichia coli* and *Streptococcus faecalis*. Moreover, compounds **3k**, **3l**, **4c**, **4g**, and **4j** have been found to kill HepG2, MDA-MB-231, MCF7, RMS, and C26 cancer cells with low μM IC$_{50}$ (2.39–10.95). These compounds showed comparable drug-like properties as ciprofloxacin, fluconazole, and paclitaxel in computational ADMET profiling. Finally, docking studies were used to assess potential protein targets responsible for their biological activities. Especially, we found that DHFR is a promising target both *in silico* and *in vitro* with compound **4c** having IC$_{50}$ of 2.35 μM.

1. Introduction

Heterocyclic compounds, which are present in a large number of biologically active synthetic and natural substances including many drugs, are of interest to pharmaceutical chemists for designing new potential bioactive compounds with a wide range of biological activities.[1,2] Benzimidazole is a naturally occurring bicyclic compound consisting of fused benzene and imidazole ring and is an integral part of the structure of vitamin B$_{12}$. Moreover, benzimidazole derivatives have showed anticancer,[1,3–5] antimicrobial,[4,6–8] anti-inflammation,[9] antiviral,[10] antihypertensive,[11] antihistamine,[12] antitubercular,[13] antiulcer,[14] analgesic,[15] anthelmintic,[16] antiprotozoal,[17] antiamoebic,[18] anticonvulsant,[19] antiparasitic.[20] In addition, benzimidazole scaffold presents in core structure of a vast list of important drugs such as antiulcer (omeprazole, lansoprazole, rabeprazole, pantoprazole), antihistamines (astemizole, clemizole, and emedastine), antihypertensives (telmisartan, candesartan, and azilsartan), anthelmintics (thiabendazole, parbendazole, mebendazole, albendazole, cambendazole, and

^{a}Department of Medicinal Chemistry, Faculty of Pharmacy, Hong Bang International University, 700000 Ho Chi Minh City, Vietnam. E-mail: canhem112009@gmail.com; empc@hiu.vn

^{b}Department of Pharmacology – Clinical Pharmacy, Faculty of Pharmacy, City Children's Hospital, 700000 Ho Chi Minh City, Vietnam

^{c}Department of Pharmacognosy & Botany, Faculty of Pharmacy, Hong Bang International University, 700000 Ho Chi Minh City, Vietnam

^{d}School of Biomedical Engineering, International University, 700000 Ho Chi Minh City, Vietnam. E-mail: vblong@hcmiu.edu.vn

^{e}Vietnam National University Ho Chi Minh City (VNU-HCM), Ho Chi Minh 700000, Vietnam

^{f}Department of Microbiology – Parasitology, Faculty of Pharmacy, University of Medicine and Pharmacy at Ho Chi Minh City, 700000 Ho Chi Minh City, Vietnam

^{g}Uppsala University, Sweden and Tra Vinh University, Vietnam

^{h}Department of Organic Chemistry, Faculty of Pharmacy, University of Medicine and Pharmacy at Ho Chi Minh City, 700000 Ho Chi Minh City, Vietnam. E-mail: lnbkhanh@ump.edu.vn; truongtuyen@ump.edu.vn

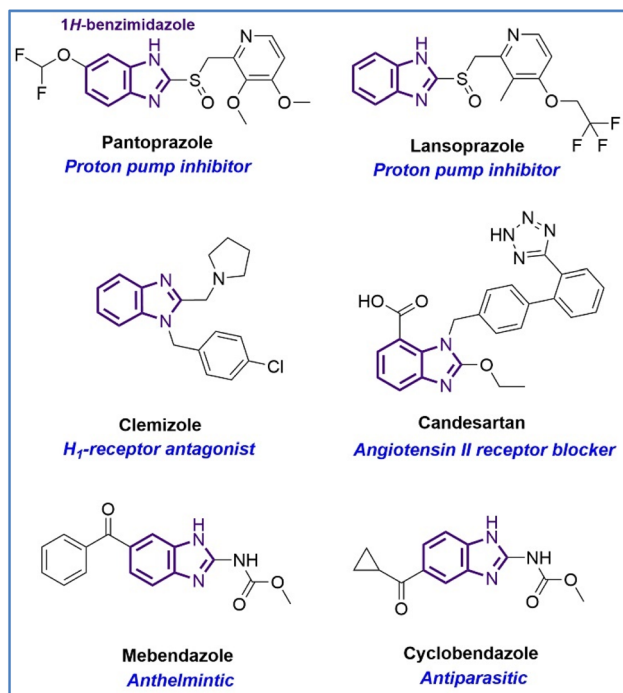† Electronic supplementary information (ESI) available. See DOI: https://doi.org/10.1039/d2ra06667j

Fig. 1 Several drug compounds containing 1*H*-benzimidazole moiety.

Fig. 2 Rational study design of *N*,2,6-trisubstituted 1*H*-benzimidazole derivatives (MIC − minimal inhibitory concentration).

flubendazole), antiviral (maribavir), antiparasitic (cyclobendazole, luxabendazole, and cambendazole), antidiabetic (rivoglitazone), analgesic (clonitrazene), especially antifungal (systemic fungicide, *e.g.* benomyl) and anticancer (antimitotic agent, *e.g.* nocodazole, PARP inhibitor, *e.g.* veliparib).[21] Furthermore, the potency of drugs like carbendazim,[22] and dovitinib containing benzimidazole moiety has been recognized against various types of cancer cell lines (Fig. 1).[23]

1*H*-Benzimidazole structures with different substituents at positions C-2 and C-5/6 can be synthesized by different methods. However, the most efficient syntheses are the condensation of *o*-phenylenediamines with carboxylic acids (or their derivatives such as nitriles, chlorides, and orthoesters) in the presence of an acid or with aldehydes using sodium metabisulfite ($Na_2S_2O_5$).[1,5] In addition, N-1 substituent 1*H*-benzimidazole derivatives can be introduced by *N*-alkylation with substituted halides in the presence of a base.[24] Our study highlights the use of the green and environmentally-friendly chemical method as using microwaves in the whole synthesis process of 1*H*-benzimidazole derivatives.

Rationale and structure-based design of new antimicrobial and anticancer agents: Structure–activity relationship studies of the benzimidazole ring system suggested that the N-1, C-2, and C-6 positions are important for biological activities.[25,26] Especially, the N-1 position can increase anticancer activity when attached to different substituents, for example, benzyl groups similar to clemizole and candesartan drugs. As part of our ongoing research, we were interested in designing *N*-substituted benzimidazoles which were presented in many biologically active compounds.[24,27] Our designed derivatives and Dovitinib anticancer drug, Benomyl antifungal drug, and antibacterial
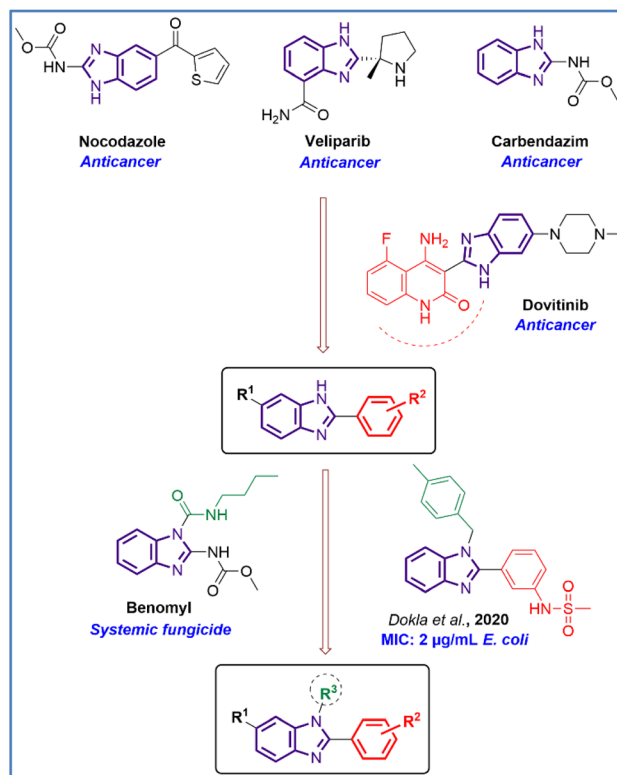
derivatives of Dokla *et al.*, 2020 (MIC on *E. coli* strain of 2 μg mL^{-1}) share three common essential structural features: a planar benzimidazole moiety, C-2 aromatic substitution, and N-1 substitution.[28] Moreover, the C-6 position with different substituents such as –H and –CH$_3$ were designed in order to examine their effects on antimicrobial and anticancer activities (Fig. 2).

Mechanistically, one pharmacological activity can be linked to one or more different receptors.[2,29] A receptor may also be involved in different biological activities. Furthermore, the mechanism of action on the cell membrane and the inhibition of important enzymes present in both microbial and cancer cells may confer dual antibacterial, antifungal, and antitumor effects. A good example is dihydrofolate reductase (DHFR) which is a potential receptor for both antitumor and antimicrobial activities.[21,30] This could be due to the similarity of DHFR from bacteria, fungi, and the cancer cell line. Therefore, the *in silico* studies were the potential approach to confirm the ligand–target interaction in many different receptors. In recent years there has been significant progress to improve the receptor flexibility in docking,[31–33] *in silico* studies are able to rank the compound potency or precisely predict the target after having experimental *in vitro* results.

The development of antibiotic resistance in microorganisms, as well as cancer resistance, has resulted in research and development in search of new antibiotics and anticancer drugs to maintain an effective drug supply at all times. It is important to find out newer, safer, and more effective antibiotics and

anticancer drugs with multiple effects, especially showing good anticancer and anti-microbial activities. This is very beneficial for cancer patients due to their weakened immunity and susceptibility to microbial attack. Therefore, the purpose of this study is to synthesize novel *N*,2,6-trisubstituted 1*H*-benzimidazole derivatives with various substituents at positions N-1, C-2, and C-6 and evaluation of their antibacterial, antifungal, and anticancer activities in continuation of our recent study.[4]

2. Results and discussion

2.1. Chemistry

The benzene-1,2-diamine derivatives with a 4-H or 4-CH$_3$ group are the starting material for the preparation of *N*,2,6-trisubstituted 1*H*-benzimidazole derivatives. The process of synthetic research consists of two steps (Scheme 1). Firstly, a series of 2,6-disubstituted 1*H*-benzimidazole derivatives (**1a–1w** and **2a–2w**) have been synthesized by condensing benzene-1,2-diamine derivatives with substituted aromatic aldehydes using conventional heating and microwave-assisted methods. Forty-six derivatives have been synthesized in good to excellent yields with the reflux method (75 to 93%) and excellent yields with the microwave-assisted method (90 to 99%). The reaction time has been dramatically reduced, as using conventional heating the reaction is carried out in 6–12 h compared with 10–15 min heating in the microwave. In addition, the reaction yield has increased ranging between 6 to 17% with microwave assistance (Table 1). Secondly, a series of *N*,2,6-trisubstituted 1*H*-benzimidazole derivatives (**3a–3l** and **4a–4k**) have been synthesized by reacting 2,6-disubstituted 1*H*-benzimidazole derivatives with substituted halides using conventional heating and microwave-assisted methods. Compounds **3a–3l** showed about 2 times higher yields than compounds **4a–4k**. Twenty-three derivatives have been synthesized in moderate to good yields with the reflux method (35 to 86%) and moderate to excellent yields with the microwave-assisted method (46 to 98%). The reaction time also has been dramatically reduced, as using conventional heating the reaction is carried out in 12–24 h compared with 20–60 min heating in the microwave. Furthermore, the reaction

yield has increased ranging between 3 to 20% with microwave assistance (Table 2). The synthesized compounds possess physical–chemical properties of fragments (M. Wt around 250) or lead-like (M. Wt around 350) that follow Lipinski's rules which is an excellent starting point for further development.[34,35] Especially, sixteen derivatives (**3b–3d**, **3g**, **3j**, and **4a–4k**) are new compounds.

Structures of synthesized compounds were assigned using IR, ^{1}H NMR, ^{13}C NMR, and mass spectroscopies. In IR spectra, the medium absorbance band of the aromatic ring (ν 1520–1395 cm^{-1} region), as well as a strong absorbance band of imine (C=N) of imidazole nucleus of 1*H*-benzimidazole derivatives (ν 1650–1510 cm^{-1} region), were observed. In addition, in ^{1}H NMR spectra of compounds **1** and **2** in DMSO characteristic chemical shifts of NH protons of 1*H*-benzimidazole (singlet in the δ 13.35–12.30 ppm region) and aromatic protons (in the δ 9.35–6.70 ppm region) were observed. On the other hand, ^{1}H NMR spectra of compounds **3** and **4** revealed the appearance of a singlet in the 5.80–4.85 ppm region of the –CH$_2$–CH=CH$_2$ or –CH$_2$–Ar group. Furthermore, the C=N group (δ 153.5–142.5 ppm) and the –CH$_2$–CH=CH$_2$ or –CH$_2$–Ar group (δ 48.0–45.5 ppm) were identified in the ^{13}C NMR spectrum of compounds **3** and **4**. Finally, mass spectra showed the molecular ion peak M (m/z) of compounds **1–4** which helped to confirm the hypothesized structure.

2.2. *In vitro* antibacterial and antifungal activities

Antimicrobial activities (exhibited by MIC values) including antibacterial activities against two strains of Gram-negative (EC – *Escherichia coli* and PA – *Pseudomonas aeruginosa*) and three strains of Gram-positive (SF – *Streptococcus faecalis*, MSSA, MRSA) and antifungal activities (CA – *Candida albicans* and AN – *Aspergillus niger*) of all synthesized compounds are summarized in Tables 3 and 4. In antimicrobial evaluation, a series of 2,6-disubstituted 1*H*-benzimidazole derivatives were inactive against Gram-negative strain PA (MIC $\geq$ 1024 μg mL^{-1}). Compounds **1a–1n**, **1p–1w**, **2a–2c**, **2e–2n**, and **2p–2w** showed weak to moderate activities against 4 strains of bacteria (EC, SF, MSSA, and MRSA) and 2 strains of fungi (MIC $\geq$ 32 μg mL^{-1}). Compound **1o** (4-methylthio) showed good antibacterial activities against the Gram-positive strains MSSA and MRSA with MIC ranging between 16 to 32 μg mL^{-1} as compared to ciprofloxacin (Cipro, MIC = 8–16 μg mL^{-1}), but showed moderate activities against the strains EC, SF, CA, and AN (MIC 64 μg mL^{-1}). In addition, compounds **2d** (3,4-dichloro) and **2o** (4-methylthio) showed good antibacterial activities against the Gram-positive strains SF, MSSA, and MRSA with MIC of 16, 16, and 32 μg mL^{-1}, respectively as compared to Cipro (MIC = 8–16 μg mL^{-1}). However, these compounds showed moderate activities against the strains EC, CA, and AN (MIC 32–64 μg mL^{-1}). The results suggested that the 4-methylthio group of the aromatic ring at position 2 of the 1*H*-benzimidazole scaffold enhanced antibacterial activities against MSSA and MRSA strains.

With antimicrobial activities of series of *N*,2,6-trisubstituted 1*H*-benzimidazole derivatives, compounds **3a–3e**, **3h–3j**, **4a**, **4b**, **4d–4f**, **4h**, **4i**, and **4k** showed weak to moderate activities against
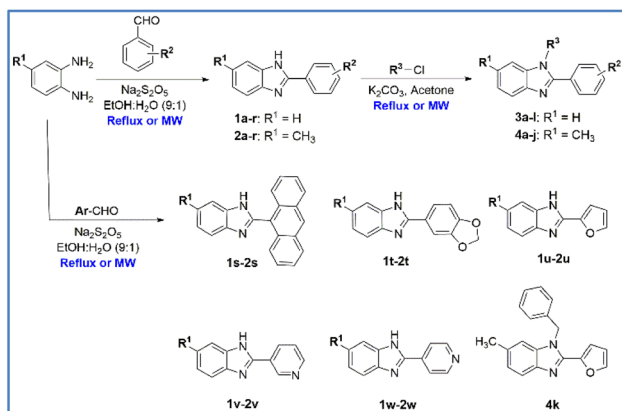
Scheme 1 Synthesis of *N*,2,6-trisubstituted 1*H*-benzimidazole derivatives (MW: microwave irradiation, EtOH: ethanol).

Table 1 Yields and physicochemical parameters of 2,6-disubstituted 1H-benzimidazole derivatives (**1a–1w** and **2a–2w**)[a]

Entry	R¹	R²	Code	Physicochemical parameters		Re	MW
1	6-H	2-Cl	**1a**	M. Wt: 228.68 NHA: 1 NHD: 1	NRB: 1, log P: 3.39 TPSA: 28.68	81	94
2	6-H	4-Cl	**1b**	M. Wt: 228.68, NHA: 1, NHD: 1	NRB: 1, log P: 3.48, TPSA: 28.68	75	90
3	6-H	2,4-Cl$_2$	**1c**	M. Wt: 263.12, NHA: 1, NHD: 1	NRB: 1, log P: 3.95, TPSA: 28.68	80	92
4	6-H	3,4-Cl$_2$	**1d**	M. Wt: 263.12, NHA: 1, NHD: 1	NRB: 1, log P: 3.99, TPSA: 28.68	87	95
5	6-H	2-Cl, 6-F	**1e**	M. Wt: 246.67, NHA: 2, NHD: 1	NRB: 1, log P: 3.75, TPSA: 28.68	82	98
6	6-H	3,4-(OCH$_3$)$_2$	**1f**	M. Wt: 254.28, NHA: 3, NHD: 1	NRB: 3, log P: 2.88, TPSA: 47.14	77	91
7	6-H	4-OC$_2$H$_5$	**1g**	M. Wt: 238.28, NHA: 2, NHD: 1	NRB: 3, log P: 3.23, TPSA: 37.91	78	90
8	6-H	3-OC$_2$H$_5$, 4-OH	**1h**	M. Wt: 254.28, NHA: 3, NHD: 2	NRB: 3, log P: 2.87, TPSA: 58.14	83	92
9	6-H	4-F	**1i**	M. Wt: 212.22, NHA: 2, NHD: 1	NRB: 1, log P: 3.25, TPSA: 28.68	89	98
10	6-H	2-OH	**1j**	M. Wt: 210.23, NHA: 2, NHD: 2	NRB: 1, log P: 2.60, TPSA: 48.91	79	90
11	6-H	2-OH, 5-Br	**1k**	M. Wt: 289.13, NHA: 2, NHD: 2	NRB: 1, log P: 3.16, TPSA: 48.91	80	97
12	6-H	3-OH	**1l**	M. Wt: 210.23, NHA: 2, NHD: 2	NRB: 1, log P: 2.53, TPSA: 48.91	85	98
13	6-H	3-OH, 4-OCH$_3$	**1m**	M. Wt: 240.26, NHA: 3, NHD: 2	NRB: 2, log P: 2.53, TPSA: 58.14	87	98
14	6-H	3-OCH$_3$	**1n**	M. Wt: 224.26, NHA: 2, NHD: 1	NRB: 2, log P: 2.94, TPSA: 37.91	80	94
15	6-H	4-SCH$_3$	**1o**	M. Wt: 240.32, NHA: 1, NHD: 1	NRB: 2, log P: 3.49, TPSA: 53.98	76	91
16	6-H	3-NO$_2$	**1p**	M. Wt: 239.23, NHA: 3, NHD: 1	NRB: 2, log P: 2.31, TPSA: 74.50	84	94
17	6-H	4-NO$_2$	**1q**	M. Wt: 239.23, NHA: 3, NHD: 1	NRB: 2, log P: 2.31, TPSA: 74.50	93	99
18	6-H	4-N(CH$_3$)$_2$	**1r**	M. Wt: 237.30, NHA: 1, NHD: 1	NRB: 2, log P: 2.94, TPSA: 31.92	80	90
19	6-H		**1s**	M. Wt: 294.35, NHA: 1, NHD: 1	NRB: 1, log P: 4.69, TPSA: 28.68	86	97
20	6-H		**1t**	M. Wt: 238.24, NHA: 3, NHD: 1	NRB: 1, log P: 2.76, TPSA: 47.14	85	98
21	6-H		**1u**	M. Wt: 184.19, NHA: 2, NHD: 1	NRB: 1, log P: 2.28, TPSA: 41.82	81	96
22	6-H		**1v**	M. Wt: 195.22, NHA: 2, NHD: 1	NRB: 1, log P: 2.20, TPSA: 41.57	79	91
23	6-H		**1w**	M. Wt: 195.22, NHA: 2, NHD: 1	NRB: 1, log P: 2.19, TPSA: 41.57	77	90
24	6-CH$_3$	2-Cl	**2a**	M. Wt: 242.70, NHA: 1, NHD: 1	NRB: 1, log P: 3.77, TPSA: 28.68	93	99
25	6-CH$_3$	4-Cl	**2b**	M. Wt: 242.70, NHA: 1, NHD: 1	NRB: 1, log P: 3.82, TPSA: 28.68	87	97
26	6-CH$_3$	2,4-Cl$_2$	**2c**	M. Wt: 277.15, NHA: 1, NHD: 1	NRB: 1, log P: 4.27, TPSA: 28.68	85	91
27	6-CH$_3$	3,4-Cl$_2$	**2d**	M. Wt: 277.15, NHA: 1, NHD: 1	NRB: 1, log P: 4.31, TPSA: 28.68	84	90
28	6-CH$_3$	2-Cl, 6-F	**2e**	M. Wt: 260.69, NHA: 2, NHD: 1	NRB: 1, log P: 4.12, TPSA: 28.68	83	92
29	6-CH$_3$	3,4-(OCH$_3$)$_2$	**2f**	M. Wt: 268.31, NHA: 3, NHD: 1	NRB: 3, log P: 3.21, TPSA: 47.14	75	90
30	6-CH$_3$	4-OC$_2$H$_5$	**2g**	M. Wt: 252.31, NHA: 2, NHD: 1	NRB: 3, log P: 3.61, TPSA: 37.91	83	90
31	6-CH$_3$	3-OC$_2$H$_5$, 4-OH	**2h**	M. Wt: 268.31, NHA: 3, NHD: 2	NRB: 3, log P: 3.22, TPSA: 58.14	78	91
32	6-CH$_3$	4 F	**2i**	M. Wt: 226.25, NHA: 2, NHD: 1	NRB: 1, log P: 3.59, TPSA: 28.68	82	93
33	6-CH$_3$	2-OH	**2j**	M. Wt: 224.26, NHA: 2, NHD: 2	NRB: 1, log P: 2.93, TPSA: 48.91	85	94
34	6-CH$_3$	2-OH, 5-Br	**2k**	M. Wt: 303.15, NHA: 2, NHD: 2	NRB: 1, log P: 3.55, TPSA: 48.91	86	95
35	6-CH$_3$	3-OH	**2l**	M. Wt: 224.26, NHA: 2, NHD: 2	NRB: 1, log P: 2.87, TPSA: 48.91	85	95
36	6-CH$_3$	3-OH, 4-OCH$_3$	**2m**	M. Wt: 254.28, NHA: 3, NHD: 2	NRB: 2, log P: 2.84, TPSA: 58.14	78	92
37	6-CH$_3$	3-OCH$_3$	**2n**	M. Wt: 238.28, NHA: 2, NHD: 1	NRB: 2, log P: 3.27, TPSA: 37.91	76	90
38	6-CH$_3$	4-SCH$_3$	**2o**	M. Wt: 254.35, NHA: 1, NHD: 1	NRB: 2, log P: 3.80, TPSA: 53.98	75	90
39	6-CH$_3$	3-NO$_2$	**2p**	M. Wt: 253.26, NHA: 3, NHD: 1	NRB: 2, log P: 2.65, TPSA: 74.50	88	94
40	6-CH$_3$	4-NO$_2$	**2q**	M. Wt: 253.26, NHA: 3, NHD: 1	NRB: 2, log P: 2.65, TPSA: 74.50	90	98
41	6-CH$_3$	4-N(CH$_3$)$_2$	**2r**	M. Wt: 251.33, NHA: 1, NHD: 1	NRB: 2, log P: 3.31, TPSA: 31.92	77	91
42	6-CH$_3$		**2s**	M. Wt: 308.38, NHA: 1, NHD: 1	NRB: 1, log P: 5.01, TPSA: 28.68	81	92
43	6-CH$_3$		**2t**	M. Wt: 252.27, NHA: 3, NHD: 1	NRB: 1, log P: 3.09, TPSA: 47.14	83	95
44	6-CH$_3$		**2u**	M. Wt: 198.22, NHA: 2, NHD: 1	NRB: 1, log P: 2.62, TPSA: 41.82	75	90
45	6-CH$_3$		**2v**	M. Wt: 209.25, NHA: 2, NHD: 1	NRB: 1, log P: 2.50, TPSA: 41.57	77	90
46	6-CH$_3$		**2w**	M. Wt: 209.25, NHA: 2, NHD: 1	NRB: 1, log P: 2.52, TPSA: 41.57	87	98

[a] Re and MW – yields of conventional heating (or reflux) and microwave-assisted method (%), Re – reflux, MW – microwave, M. Wt – molecular weight, NHA – number of hydrogen bond acceptor, NHD – number of hydrogen bond donor, NRB – number rotatable bond, PSA – polar surface area (Angstroms squared).

5 strains of bacteria and 2 strains of fungi (MIC ≥ 32 μg mL⁻¹). Compounds **3f** (3,4-dichloro, N-benzyl), **3l** (4-chloro, N-(4-chlorobenzyl)), and **4g** (4-nitro, N-Benzyl) showed good antibacterial activities against the Gram-positive strains MSSA and MRSA with MIC of 8 and 16 μg mL⁻¹, respectively. Compound **3f** showed weak antimicrobial activities against strains EC, SF, CA, and AN with MIC ≥ 64 μg mL⁻¹. Compound **3l** showed good antimicrobial activities against strains EC, SF, CA, and AN with

MIC ranging between 16 to 32 μg mL⁻¹ and weak antibacterial activity against the Gram-negative strain PA with a MIC value of 256 μg mL⁻¹. Compound **4g** showed good antimicrobial activity against strain SF with MIC of 8 μg mL⁻¹ as compared to Cipro (MIC = 8 μg mL⁻¹) and weak antimicrobial activity against the strains EC, PA, CA, and AN with MIC ≥ 64 μg mL⁻¹. Moreover, compounds **3g** (3,4-dimethoxy, N-benzyl), **3k** (4-nitro, N-benzyl), **4c** (4-chloro, N-benzyl), and **4j** (4-nitro, N-(4-chlorobenzyl))

Table 2 Yields and physicochemical parameters of N,2,6-trisubstituted 1H-benzimidazole derivatives (3a–3l and 4a–4k)[a]

Entry	R groups			Code	Physicochemical parameters		Yield	
	R^1	R^2	R^3				Re	MW
1	6-H	4-Cl	Allyl	3a	M. Wt: 268.74 NHA: 1 NHD: 0	NRB: 3, log P: 4.05 TPSA: 17.82	82	98
2	6-H	3,4-Cl$_2$	Allyl	3b	M. Wt: 303.19, NHA: 1, NHD: 0	NRB: 3, log P: 4.56, TPSA: 17.82	76	94
3	6-H	3,4-(OCH$_3$)$_2$	Allyl	3c	M. Wt: 294.35, NHA: 3, NHD: 0	NRB: 5, log P: 3.48, TPSA: 36.28	72	92
4	6-H	4-NO$_2$	Allyl	3d	M. Wt: 279.29, NHA: 3, NHD: 0	NRB: 4, log P: 2.90, TPSA: 63.64	86	98
5	6-H	4-Cl	Benzyl	3e	M. Wt: 318.80, NHA: 1, NHD: 0	NRB: 3, log P: 4.73, TPSA: 17.82	82	94
6	6-H	3,4-Cl$_2$	Benzyl	3f	M. Wt: 353.24, NHA: 1, NHD: 0	NRB: 3, log P: 5.27, TPSA: 17.82	74	94
7	6-H	3,4-(OCH$_3$)$_2$	Benzyl	3g	M. Wt: 344.41, NHA: 3, NHD: 0	NRB: 5, log P: 4.16, TPSA: 36.28	76	96
8	6-H	4-OC$_2$H$_5$	Benzyl	3h	M. Wt: 328.41, NHA: 2, NHD: 0	NRB: 5, log P: 4.51, TPSA: 27.05	70	88
9	6-H	4-F	Benzyl	3i	M. Wt: 302.34, NHA: 2, NHD: 0	NRB: 3, log P: 4.51, TPSA: 17.82	82	98
10	6-H	3-OCH$_3$	Benzyl	3j	M. Wt: 314.38, NHA: 2, NHD: 0	NRB: 4, log P: 4.21, TPSA: 27.05	78	96
11	6-H	4-NO$_2$	Benzyl	3k	M. Wt: 329.35, NHA: 3, NHD: 0	NRB: 4, log P: 3.59, TPSA: 63.64	84	96
12	6-H	4-Cl	4-Chlorobenzyl	3l	M. Wt: 353.24, NHA: 1, NHD: 0	NRB: 3, log P: 5.24, TPSA: 17.82	80	98
13	6-CH$_3$	4-Cl	Allyl	4a	M. Wt: 282.77, NHA: 1, NHD: 0	NRB: 3, log P: 4.39, TPSA: 17.82	42	50
14	6-CH$_3$	4-NO$_2$	Allyl	4b	M. Wt: 293.32, NHA: 3, NHD: 0	NRB: 4, log P: 3.21, TPSA: 63.64	41	47
15	6-CH$_3$	4-Cl	Benzyl	4c	M. Wt: 332.83, NHA: 1, NHD: 0	NRB: 3, log P: 5.08, TPSA: 17.82	42	48
16	6-CH$_3$	3,4-Cl$_2$	Benzyl	4d	M. Wt: 367.27, NHA: 1, NHD: 0	NRB: 3, log P: 5.58, TPSA: 17.82	45	49
17	6-CH$_3$	4-F	Benzyl	4e	M. Wt: 316.37, NHA: 2, NHD: 0	NRB: 3, log P: 4.84, TPSA: 17.82	43	46
18	6-CH$_3$	4-SCH$_3$	Benzyl	4f	M. Wt: 344.47, NHA: 1, NHD: 0	NRB: 4, log P: 5.05, TPSA: 43.12	44	50
19	6-CH$_3$	4-NO$_2$	Benzyl	4g	M. Wt: 343.38, NHA: 3, NHD: 0	NRB: 4, log P: 3.89, TPSA: 63.64	42	50
20	6-CH$_3$	4-Cl	2-Chlorobenzyl	4h	M. Wt: 367.27, NHA: 1, NHD: 0	NRB: 3, log P: 5.55, TPSA: 17.82	43	48
21	6-CH$_3$	4-NO$_2$	2-Chlorobenzyl	4i	M. Wt: 377.82, NHA: 3, NHD: 0	NRB: 4, log P: 4.39, TPSA: 63.64	39	49
22	6-CH$_3$	4-NO$_2$	4-Chlorobenzyl	4j	M. Wt: 377.82, NHA: 3, NHD: 0	NRB: 4, log P: 4.42, TPSA: 63.64	35	46
23	6-CH$_3$		Benzyl	4k	M. Wt: 288.34, NHA: 2, NHD: 0	NRB: 3, log P: 3.82, TPSA: 30.96	36	47

[a] Re and MW – yields of conventional heating (or reflux) and microwave-assisted method (%), Re – reflux, MW – microwave, M. Wt – molecular weight, NHA – number of hydrogen bond acceptor, NHD – number of hydrogen bond donor, NRB – number rotatable bond, PSA – polar surface area (Angstroms squared).

exhibited the strongest activity among the synthesized compounds against the Gram-positive strains MSSA and MRSA with MIC ranging between 4 to 8 μg mL^{-1} as compared to Cipro. However, compounds 3g, 3k, and 4c showed weak to moderate activities against strains EC, PA, SF, CA, and AN. In contrast, compound 4c showed good antimicrobial activities against the bacteria strains EC, SF, and the fungi strain CA with the MIC value of 16 μg mL^{-1} as compared to ciprofloxacin and fluconazole (Flu, MIC of 4 μg mL^{-1}), except for showed moderate antibacterial activity against Gram-negative strain PA. In particular, for antifungal activity, compound 4c also displayed promising activity against *Aspergillus niger* with the MIC value of 32 μg mL^{-1} as compared to Flu (MIC = 128 μg mL^{-1}). From the structure–activity relationship (SAR), the presence of the *N*-benzyl group and the chloro/nitro group in the aromatic ring at position 2 of the 1*H*-benzimidazole scaffold is more desirable for enhanced antibacterial activity in 3f, 3l, 3k, 4c, and 4j, and antifungal activity in 3l and 4c (Fig. 3).

In published studies, 4-substituent 5,6-dichloro-1*H*-benzimidazole derivatives showed antibacterial activity against *S. aureus* with MIC 3.12 mg mL^{-1}.[6] Besides, the 4-nitro 1*H*-benzimidazole-5-carbohydrazide derivative exhibited good inhibitory activity against lanosterol 14α-demethylase (CYP51) with IC$_{50}$ value at 0.19 μg mL^{-1} compared to fluconazole as reference IC$_{50}$ value at 0.62 μg mL^{-1}.[36] In addition, the pyridin-3-yl-1*H*-benzimidazole-5-carboxylate derivative was found to be potent activity against *Mycobacterium tuberculosis* H37Rv and

INH-resistant *Mycobacterium tuberculosis* with MIC value of 0.112 μM and 6.12 μM, respectively.[37] Especially, the 6-fluoro-1*H*-benzimidazole derivative showed potent antibacterial activities against the Gram-positive strains MSSA (MIC of 4 μg mL^{-1}) and MRSA (MIC of 2–8 μg mL^{-1}).[8] Two synthesized compounds 3k and 4c with 2-(4-nitro/chloro-phenyl) moiety also exhibited potent antibacterial activity with MICs of 4–8 μg mL^{-1} against MSSA and MSRA strains. This may be due to the structure of compound 3k with the presence of a 4-nitro group on the phenyl ring of the 1*H*-benzimidazole nucleus is similar to that of Morcoss *et al.* (2020) and the structure of compound 4c with the presence of 4-chloro group on the phenyl ring of the 1*H*-benzimidazole nucleus is similar to that of Tunçbilek *et al.* (2009) and Em *et al.* (2022).[4,6,36] However, compounds 3k and 4c have different substituent patterns compared to our previous most potent compounds.[4]

2.3. Anticancer activity

Next, we assessed the anticancer activity of compounds 1a–1w, 2a–2w, 3a–3l, and 4a–4k on five cancer cell lines hepatocellular carcinoma cell line (HepG2), human breast cancer cell lines (MDA-MB-231 and MCF7), the aggressive and highly malignant rhabdomyosarcoma cell line (RMS), and colon carcinoma cell line (C26) using paclitaxel (PTX) as a non-selective positive control in MTT assay. The results are summarized in Tables 3 and 4

Table 3 Antimicrobial (MIC, µg mL^{-1}) and anticancer (IC$_{50}$, µM) activities of synthesized compounds 1a–1w and 2a–2w[a]

Entry	Code	Antibacterial					Antifungal		Anticancer				
		EC	PA	SF	MSSA	MRSA	CA	AN	HepG2	MDA-MB-231	MCF7	RMS	C26
1	**1a**	—	—	—	64	128	512	512	31.50 ± 1.34	50.31 ± 2.52	69.02 ± 2.18	42.44 ± 1.98	35.81 ± 1.45
2	**1b**	—	—	—	64	128	256	256	51.46 ± 6.27	>100	67.12 ± 1.63	>100	78.93 ± 2.86
3	**1c**	128	—	64	128	256	—	—	37.50 ± 1.60	52.16 ± 3.02	55.76 ± 2.05	35.01 ± 2.47	28.90 ± 1.54
4	**1d**	32	—	32	32	64	256	256	**7.45 ± 1.72**	**9.83 ± 1.56**	**11.08 ± 1.44**	**10.41 ± 1.06**	**6.43 ± 1.35**
5	**1e**	64	—	—	64	128	—	—	>100	68.95 ± 2.54	>100	>100	63.78 ± 2.67
6	**1f**	—	—	—	128	256	—	—	44.06 ± 4.73	50.05 ± 2.81	>100	>100	43.59 ± 2.64
7	**1g**	—	—	—	256	512	—	—	43.08 ± 2.97	>100	>100	25.07 ± 1.43	>100
8	**1h**	—	—	256	128	256	512	512	42.51 ± 2.24	48.26 ± 4.02	59.25 ± 2.65	29.38 ± 1.89	31.93 ± 2.77
9	**1i**	256	—	—	256	512	—	—	35.82 ± 3.36	>100	68.03 ± 3.14	>100	26.07 ± 1.66
10	**1j**	—	—	—	256	256	—	—	68.26 ± 3.01	35.94 ± 2.34	>100	15.37 ± 0.97	50.53 ± 2.85
11	**1k**	64	—	128	64	128	512	512	**8.94 ± 1.66**	**12.83 ± 2.45**	**5.10 ± 1.43**	**7.25 ± 1.41**	**6.81 ± 1.23**
12	**1l**	64	—	64	64	128	—	—	83.02 ± 3.59	>100	>100	73.80 ± 2.55	>100
13	**1m**	256	—	64	128	256	256	512	64.22 ± 2.97	88.13 ± 2.45	29.67 ± 1.24	53.05 ± 2.07	66.38 ± 2.31
14	**1n**	256	—	—	256	512	—	—	47.13 ± 4.69	25.47 ± 1.43	51.38 ± 2.55	79.05 ± 3.96	28.78 ± 1.95
15	**1o**	64	—	64	16	32	64	64	40.05 ± 1.32	36.59 ± 1.14	33.18 ± 1.71	21.56 ± 1.19	37.44 ± 2.08
16	**1p**	—	—	—	64	64	512	512	39.03 ± 3.28	>100	24.41 ± 1.12	50.34 ± 3.81	42.66 ± 2.79
17	**1q**	128	—	64	128	256	512	512	21.04 ± 2.87	26.89 ± 1.38	27.22 ± 2.35	23.45 ± 1.27	21.89 ± 2.42
18	**1r**	64	—	64	64	128	256	512	37.49 ± 2.36	29.07 ± 1.66	>100	50.51 ± 2.04	61.52 ± 3.29
19	**1s**	64	—	64	32	64	256	256	**9.79 ± 0.78**	**8.40 ± 1.13**	**13.20 ± 1.07**	**7.66 ± 1.05**	**8.15 ± 0.94**
20	**1t**	—	—	—	128	256	—	—	>100	>100	>100	>100	>100
21	**1u**	ND	ND	ND	ND	ND	ND	ND	ND	ND	ND	ND	ND
22	**1v**	64	—	64	128	256	—	—	70.61 ± 2.93	>100	>100	87.72 ± 3.71	>100
23	**1w**	128	—	—	128	256	—	—	87.72 ± 3.46	>100	>100	31.25 ± 2.09	>100
24	**2a**	64	—	256	64	256	512	—	95.58 ± 4.23	64.94 ± 2.80	>100	46.49 ± 2.33	36.70 ± 2.11
25	**2b**	256	—	—	256	512	256	256	28.91 ± 2.55	27.11 ± 1.48	25.62 ± 1.62	48.31 ± 2.41	18.47 ± 0.98
26	**2c**	64	—	—	64	128	—	—	30.65 ± 1.59	27.47 ± 2.05	57.24 ± 2.13	29.94 ± 1.69	34.92 ± 1.66
27	**2d**	32	—	16	16	32	32	32	56.74 ± 2.42	60.24 ± 2.70	50.81 ± 2.54	**14.41 ± 1.02**	39.36 ± 1.72
28	**2e**	128	—	128	64	64	—	—	>100	34.39 ± 1.53	>100	45.05 ± 2.01	34.59 ± 1.75
29	**2f**	64	—	128	128	256	—	—	43.57 ± 1.98	52.57 ± 1.86	>100	>100	61.08 ± 2.94
30	**2g**	—	—	—	128	256	—	—	27.40 ± 1.39	**13.23 ± 0.94**	>100	76.22 ± 2.44	32.75 ± 1.55
31	**2h**	64	—	—	32	64	—	—	77.11 ± 2.88	>100	54.89 ± 3.60	51.62 ± 2.28	19.43 ± 1.21
32	**2i**	64	—	64	64	128	512	512	80.35 ± 3.67	>100	38.62 ± 2.25	>100	15.67 ± 2.20
33	**2j**	128	—	64	128	256	256	256	26.14 ± 1.78	31.85 ± 1.90	18.04 ± 1.63	**6.76 ± 0.83**	**9.75 ± 1.25**
34	**2k**	64	—	64	64	128	256	256	**8.93 ± 1.11**	**6.69 ± 1.67**	**4.37 ± 1.09**	**10.37 ± 1.04**	69.28 ± 2.50
35	**2l**	64	—	128	32	64	128	128	95.34 ± 4.16	>100	>100	19.31 ± 1.35	52.47 ± 2.19
36	**2m**	64	—	64	64	128	512	512	59.76 ± 3.31	55.08 ± 2.44	23.70 ± 1.39	48.68 ± 2.61	34.90 ± 1.89
37	**2n**	128	—	128	128	256	256	256	26.86 ± 2.73	15.58 ± 0.99	50.63 ± 2.50	22.34 ± 1.85	33.21 ± 2.13
38	**2o**	32	—	16	16	32	64	64	>100	>100	45.01 ± 1.64	38.97 ± 1.69	47.94 ± 2.56
39	**2p**	256	—	128	64	128	256	256	71.39 ± 3.18	>100	19.20 ± 2.08	93.28 ± 2.58	19.87 ± 1.15
40	**2q**	64	—	64	128	256	512	512	18.62 ± 2.29	17.59 ± 2.23	**10.46 ± 1.44**	26.22 ± 1.88	58.33 ± 1.88
41	**2r**	64	—	64	64	128	256	256	35.07 ± 1.09	31.52 ± 2.55	47.69 ± 2.40	24.34 ± 1.65	20.02 ± 1.53
42	**2s**	128	—	64	64	128	—	—	21.40 ± 1.49	36.78 ± 2.24	39.01 ± 2.31	26.97 ± 1.42	>100
43	**2t**	—	—	—	256	512	512	—	78.95 ± 3.77	>100	>100	>100	>100
44	**2u**	128	—	256	256	256	512	512	>100	>100	>100	>100	55.08 ± 2.78
45	**2v**	128	—	64	64	128	—	—	68.37 ± 3.47	89.01 ± 2.96	51.06 ± 4.12	83.64 ± 3.81	47.05 ± 2.28
46	**2w**	64	—	64	64	128	—	—	52.63 ± 2.43	74.62 ± 2.53	54.65 ± 3.35	28.39 ± 2.17	

Table 3 (Contd.)

Entry	Code	Antibacterial					Antifungal		Anticancer				
		EC	PA	SF	MSSA	MRSA	CA	AN	HepG2	MDA-MB-231	MCF7	RMS	C26
47	**Cipro**	16	16	8	8	16	ND	ND	ND	ND	ND	ND	ND
48	**Flu**	ND	ND	ND	ND	ND	4	128	ND	ND	ND	ND	ND
49	**PTX**	ND	ND	ND	ND	ND	ND	ND	4.75 ± 0.67	1.38 ± 0.42	2.35 ± 0.51	6.13 ± 0.83	3.32 ± 0.55

^{a} MIC ≥ 1024 μg mL^{-1}, ND – not determined, EC – *Escherichia coli* ATCC 25922, PA – *Pseudomonas aeruginosa* ATCC 27853, SF – *Streptococcus faecalis* ATCC 29212, MSSA – Methicillin-susceptible strains of *Staphylococcus aureus* ATCC 29213, MRSA – Methicillin-resistant strains of *Staphylococcus aureus* ATCC 43300, CA – *Candida albicans* ATCC 10321, AN – *Aspergillus niger* ATCC 16404, Cipro – ciprofloxacin, Flu – fluconazole, MIC (μg mL^{-1}) ± 0.5 μg mL^{-1}. PTX – paclitaxel, HepG2 – human hepatocyte carcinoma cell line, MDA-MB-231 – human breast adenocarcinoma cell line, MCF7 – human breast cancer cell line, RMS – human rhabdomyosarcoma cell line, C26 – colon carcinoma cell line. IC$_{50}$ ± SEM (μM, SEM – standard error of the mean). The values in bold highlight the best compounds with the best MIC and IC$_{50}$ values compared to positive controls.

In both series of 1*H*-benzimidazole derivatives, several compounds exhibited moderate (IC$_{50}$ = 15.0–50.0 μM) or weak activity (IC$_{50}$ > 50 μM) toward HepG2, MDA-MB-231, MCF7, RMS, and C26. Compounds **2d** and **2j** showed good anticancer activity with IC$_{50}$ 14.41 and 6.76 μM, respectively as compared to PTX (IC$_{50}$ = 6.13 μM) at the RMS cell line. Compound **2g** showed moderate anticancer activity against the MDA-MB-231 cell line with an IC$_{50}$ value of 13.23 μM as compared to PTX (IC$_{50}$ = 1.38 μM). On the other hand, compound **2q** showed good anticancer activity against the MCF7 cell line with an IC$_{50}$ value of 10.46 μM as compared to PTX (IC$_{50}$ = 2.35 μM). Compound **4a** showed good anticancer activity against the C26 cell line with an IC$_{50}$ value of 9.04 μM as compared to PTX (IC$_{50}$ = 3.32 μM). Particularly, nine compounds **1d** (3,4-dichloro), **1k** (5-bromo-2-hydroxy), **1s** (Anthracen-9-yl), **2k** (5-bromo-2-hydroxy), **3k** (4-nitro, *N*-benzyl), **3l** (4-chloro, *N*-(4-chlorobenzyl)), **4c** (4-chloro, *N*-benzyl), **4g** (4-nitro, *N*-benzyl), and **4j** (4-nitro, *N*-(4-chlorobenzyl)) showed the strongest anticancer activity among the synthesized compounds against all tested cell lines with IC$_{50}$ ranging between 2.39 to 13.20 μM comparable to PTX (IC$_{50}$ = 1.38–6.13 μM). Moreover, compound **4c** showed the strongest anticancer activity among all active compounds against HepG2, MDA-MB-231, MCF7, RMS, and C26 with IC$_{50}$ of 3.22, 2.39, 5.66, 4.83, and 3.90 μM, respectively as compared to PTX. Compound **4c** exhibited a weaker anticancer activity than PTX on MDA-MB-231, MCF7, and C26 cell lines, but exhibited better anticancer activity than PTX on HepG2 and RMS cell lines (Fig. 4), and especially also showed potent antimicrobial activities (Table 4). Target engagement with electron-withdrawing substituents 4-Cl and 4-NO$_2$ on the phenyl ring, and *N*-phenyl and *N*-(4-chlorobenzyl) substituents of the 1*H*-benzimidazole scaffold may be responsible for its anticancer activity as compared to other compounds.

In published studies with similar structures, the 4-fluorophenyl benzoimidazolylquinazolinamine derivative showed potent activity against tyrosine-protein kinase Met (IC$_{50}$ of 0.05 μM) and vascular endothelial growth factor receptor 2 (VEGFR-2, IC$_{50}$ of 0.02 μM).[38] Besides, the 3,5-difluorophenyl benzimidazole–oxindole conjugate derivative exhibited 43.7% and 64.8% apoptosis against MCF-7 at 1 and 2 μM, respectively.[39] On the other hand, the 4-(*N*,*N*-dimethylamino)phenyl *N*,2,5-trisubstituted-1*H*-benzimidazole derivative exhibited Sirtuins inhibitory activity for SIRT1 and SIRT2 with IC$_{50}$ value of 54.21 and 26.85 μM, respectively. In addition, the 3-hydroxyphenyl 6-benzoyl-1*H*-benzimidazole derivative exhibited good antitumor activity against human lung adenocarcinoma epithelial (A549, IC$_{50}$ of 4.47 μM), human breast adenocarcinoma (MDA-MB-231, IC$_{50}$ of 4.68 μM), and human prostate cancer (PC3, IC$_{50}$ of 5.50 μM) cell lines.[5] Cell proliferation assay demonstrated that this compound had pronounced anticancer activity against breast MDA-MB-468, colon HCT-116, and blood-leukemia CCRF-CEM cell lines.[40] Moreover, the *N*-(3-phenylpropyl) *N*,2,5-trisubstituted-1*H*-benzimidazole derivative has been found to induce autophagy in MCF7 cells with IC$_{50}$ value of 5.73 ± 0.95 μM by fluorescence microscope assays and western blot analysis.[41] The 5-chloro-*N*-benzyl-1*H*-benzimidazole also exhibited to arrest MCF-7 cell growth at the G2/M and S phases with IC$_{50}$ value of

Table 4 Antimicrobial (MIC, µg mL^{-1}) and anticancer (IC$_{50}$, µM) activities of synthesized compounds **3a–3l** and **4a–4k**[a]

Entry	Code	Antibacterial					Antifungal				Anticancer		
		EC	PA	SF	MSSA	MRSA	CA	AN	HepG2	MDA-MB-231	MCF7	RMS	C26
1	**3a**	64	—	128	64	128	512	512	58.92 ± 3.59	73.14 ± 3.91	79.03 ± 3.30	67.39 ± 3.69	51.28 ± 3.11
2	**3b**	64	512	64	64	64	256	256	66.07 ± 3.43	40.81 ± 2.87	50.03 ± 2.99	44.48 ± 3.03	47.16 ± 2.94
3	**3c**	128	—	64	128	128	512	512	53.76 ± 3.65	31.24 ± 2.46	37.02 ± 1.95	50.38 ± 3.05	31.12 ± 2.21
4	**3d**	64	—	64	32	64	256	256	36.84 ± 3.12	43.86 ± 2.82	34.09 ± 2.67	32.60 ± 2.44	29.13 ± 2.37
5	**3e**	128	—	—	64	256	—	—	47.18 ± 4.65	35.01 ± 2.36	40.18 ± 2.70	31.65 ± 2.14	41.91 ± 2.50
6	**3f**	64	256	128	8	16	64	—	49.91 ± 3.05	52.47 ± 2.09	62.35 ± 3.14	42.78 ± 2.55	36.94 ± 2.69
7	**3g**	64	256	32	4	8	—	—	19.95 ± 3.08	27.08 ± 1.89	22.25 ± 2.01	18.37 ± 2.54	20.96 ± 2.42
8	**3h**	64	—	64	64	64	128	256	33.76 ± 3.22	21.12 ± 1.61	40.15 ± 1.90	48.64 ± 2.38	29.03 ± 2.78
9	**3i**	—	128	128	—	—	—	—	45.93 ± 3.19	34.57 ± 1.80	31.54 ± 2.35	27.96 ± 2.67	21.12 ± 1.74
10	**3j**	128	—	64	256	256	—	—	40.72 ± 3.98	43.29 ± 2.63	24.76 ± 1.81	33.02 ± 1.99	28.89 ± 1.60
11	**3k**	64	128	64	**4**	**4**	**16**	64	**7.80 ± 0.53**	**8.32 ± 0.66**	**9.56 ± 0.79**	**7.44 ± 0.81**	**10.95 ± 0.45**
12	**3l**	**16**	256	**16**	8	16	32	32	10.05 ± 0.76	7.48 ± 0.54	8.56 ± 0.83	9.67 ± 1.02	8.95 ± 0.49
13	**4a**	256	—	128	32	32	—	—	38.77 ± 2.35	30.11 ± 1.92	22.24 ± 2.60	48.81 ± 1.56	9.04 ± 0.88
14	**4b**	64	—	64	32	64	512	512	63.45 ± 3.11	>100	71.09 ± 2.84	85.97 ± 3.24	59.55 ± 2.74
15	**4c**	**16**	64	**16**	**4**	8	**16**	32	**3.22 ± 0.53**	**2.39 ± 0.54**	**5.66 ± 0.72**	**4.83 ± 0.64**	**3.90 ± 0.51**
16	**4d**	32	—	32	32	32	128	128	>100	83.25 ± 4.43	80.50 ± 3.85	78.92 ± 2.34	64.45 ± 4.11
17	**4e**	128	—	64	64	64	32	64	27.24 ± 1.48	28.54 ± 1.07	43.12 ± 2.36	35.05 ± 2.89	24.43 ± 1.78
18	**4f**	128	—	128	128	256	—	—	17.74 ± 1.37	21.87 ± 2.02	29.01 ± 2.46	31.74 ± 2.33	19.65 ± 1.85
19	**4g**	64	128	**8**	**8**	16	256	256	**6.74 ± 0.61**	**8.11 ± 0.70**	**7.86 ± 0.69**	**8.45 ± 0.90**	**7.89 ± 0.73**
20	**4h**	64	512	64	64	64	64	64	47.88 ± 4.13	74.17 ± 3.63	59.78 ± 2.50	41.03 ± 2.15	38.49 ± 3.25
21	**4i**	32	256	64	32	64	128	128	34.34 ± 3.22	28.46 ± 2.54	20.20 ± 1.93	17.61 ± 1.64	23.75 ± 2.15
22	**4j**	64	256	64	**8**	**8**	32	64	**5.53 ± 0.80**	**9.02 ± 0.68**	**6.24 ± 0.57**	**7.33 ± 0.64**	**4.95 ± 0.79**
23	**4k**	128	—	128	128	128	512	512	55.45 ± 3.32	60.51 ± 4.72	41.46 ± 4.04	39.18 ± 2.62	34.66 ± 2.01
24	Cipro	16	16	8	8	16	ND	ND	ND	ND	ND	ND	ND
25	Flu	ND	ND	ND	ND	ND	4	128	ND	ND	ND	ND	ND
26	PTX	ND	ND	ND	ND	ND	ND	ND	4.75 ± 0.67	1.38 ± 0.42	2.35 ± 0.51	6.13 ± 0.83	3.32 ± 0.55

[a] MIC ≥ 1024 µg mL^{-1}, ND – not determined, EC – *Escherichia coli* ATCC 25922, PA – *Pseudomonas aeruginosa* ATCC 27853, SF – *Streptococcus faecalis* ATCC 29212, MSSA – Methicillin-susceptible strains of *Staphylococcus aureus* ATCC 29213, MRSA – Methicillin-resistant strains of *Staphylococcus aureus* ATCC 43300, CA – *Candida albicans* ATCC 10321, AN – *Aspergillus niger* ATCC 16404, Cipro – ciprofloxacin, Flu – fluconazole, MIC (µg mL^{-1}) ± 0.5 µg mL^{-1}. PTX – paclitaxel, HepG2 – human hepatocyte carcinoma cell line, MDA-MB-231 – human breast adenocarcinoma cell line, MCF7 – human breast cancer cell line, RMS – human rhabdomyosarcoma cell line, C26 – colon carcinoma cell line. IC$_{50}$ ± SEM (µM, SEM – standard error of the mean). The values in bold highlight the best compounds with the best MIC and IC$_{50}$ values compared to positive controls.
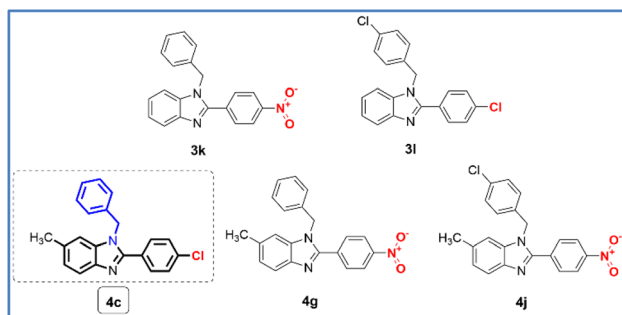
Fig. 3 The structure of potential *N*,2,6-trisubstituted 1*H*-benzimidazole derivatives.

7.01 ± 0.20 µM.[42] Similar to reported potent compounds in literature, among our most active 2,6-disubstituted 1*H*-benzimidazole derivatives **3l**, **4c**, and **4j** contain halogen substituents. This is similar to our previous most active compounds.[4] Especially, compound **4c** exhibited more potential antitumor activity against five different types of cancer cells when compared with the compounds of Yoon *et al.* (2014), Zhang *et al.* (2017), and Em *et al.* (2022).[4,40,41] This may be due to the structure of **4c** having the presence of a chlorine substituent (–Cl) at position 4 on the phenyl ring and the *N*-benzyl group on the 1*H*-benzimidazole scaffold.[4]

The development of compounds with multiple effects has been of increasing interest, especially with anticancer and antimicrobial activities. The dual-acting anticancer and antimicrobial chemotherapy agents have been published in many studies.[4,43–46] Moreover, people with cancer may have a higher risk of infection due to changes in the immune system that controls their body's defenses.[47] Therefore, our potential derivatives have shown to be promising agents in the development of dual therapeutic effects.

2.4. *In silico* ADMET profile

In this study, a computational study of all synthesized compounds was performed to determine the surface area and other physicochemical properties in the direction of Lipinski's rules (Tables 1 and 2).[4,29] The five most active compounds **3k**, **3l**, **4c**, **4g**, and **4j** follow all of Lipinski's rules. All the highest active derivatives have a number of hydrogen bonding acceptor groups ranging between 1 to 3, and nonhydrogen bonding donors. Also, molecular weights range between 329.35 to
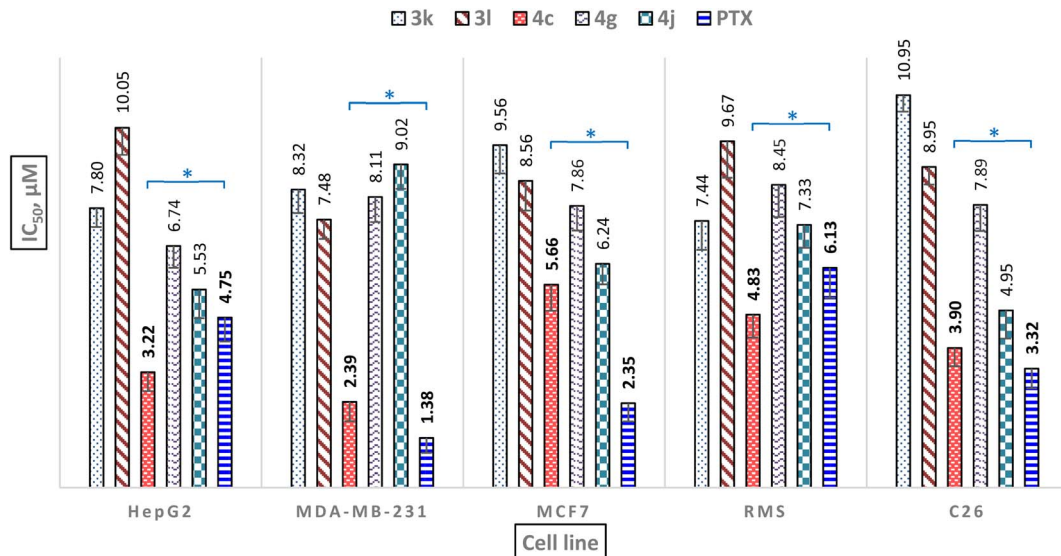
Fig. 4 Comparison of anticancer activity (IC_{50} values) between active compounds and PTX. (PTX – paclitaxel, HepG2 – human hepatocyte carcinoma cell line, MDA-MB-231 – human breast adenocarcinoma cell line, MCF7 – human breast cancer cell line, RMS – human rhabdomyosarcoma cell line, C26 – colon carcinoma cell line, (*): significantly different compared with IC_{50} of **4c** and paclitaxel with $p < 0.05$.

377.82, and $\log P$ values range between 3.59 to 5.24, and all these values agree with Lipinski's rules such as HB donor groups $\leq$ 5, HB acceptor groups $\leq$ 10, M. Wt < 500, and $\log P <$ 5.

Computational ADMET profiling of active compounds (Table S1†), showed that these derivatives have better intestinal absorption in humans than Cipro, Flu, and PTX. In fact, all compounds showed Caco-2 permeability higher than the control drugs while only compounds **3k** and **4g** showed MDCK permeability higher than the control drugs. This preference may be due to the superior lipophilic of the designed ligands, which would facilitate passage along different biological membranes.[4,29] Accordingly, they may have remarkably good bioavailability after oral administration. All compounds are highly likely to be Pgp-inhibitor similar to the PTX reference drug. This is advantageous for overcoming multidrug resistance in cancer. In addition, all compounds showed high plasma protein binding. Moreover, compound **4c** demonstrated a high potential to penetrate the blood–brain barrier (BBB), while Cipro and PTX are unable to do it. Therefore, compound **4c** showed potential for the treatment of brain tumors compared with reference drugs.

The molecule is less skin permeant, the more negative the $\log K_p$ (with Kp in cm s^{-1}). Therefore, all active compounds ($\log K_p$ in the range of -5.10 to -4.23) showed better skin permeation than Cipro ($\log K_p$ of -9.09) and Flu ($\log K_p$ of -7.92). The cytochrome enzymes could be weak to strongly inhibited under the effect of active compounds especially CYP1A2, CYP2C19, and CYP2C9, while Cipro and Flu couldn't. Compounds **3l** and **4c** also strongly inhibit CYP2D6, while PTX couldn't. However, all compounds did not show the effect of CYP3A4 inhibition compared with PTX.

The CL (clearance) is a significant parameter in deciding dose intervals as a tool for the assessment of excretion. All active compounds (5.05–6.94 mL min^{-1} kg^{-1}) and Flu (CL = 5.69 mL min^{-1} kg^{-1}) was classified as a moderate clearance level ranging between 5 to 15 mL min^{-1} kg^{-1}. In contrast, Cipro (3.21 mL min^{-1} kg^{-1}) and PTX (3.42 mL min^{-1} kg^{-1}) showed lower CL values and were classified as low clearance levels (CL < 5 mL min^{-1} kg^{-1}).

Toxicity is the last parameter examined in the ADMET profile. As displayed in Table S1,† all the new ligands did not show H-HT (human hepatotoxicity), DILI (drug-induced liver injury), rat oral acute toxicity, and eye corrosion. In particular, the most potent compound **4c** showed lower respiratory toxicity as well as the "Tox21 pathway" and "Toxicophore rules" properties better than the reference drugs.

2.5. *In silico* molecular docking studies

Following ADMET profiling, docking was used to assess the potential targets for the most active compounds. Based on the principle that similar compounds tend to bind to the same proteins as well as *in vitro* enzymes inhibition of the reported homologous benzimidazole structures, seven protein targets were chosen for docking study for the five most active compounds and reference compounds (Cipro – ciprofloxacin, Flu – fluconazole, and PTX – paclitaxel).[4] Four different target proteins were selected for antimicrobial activity including dihydrofolate reductase (DHFR-F) and *N*-myristoyl transferase (NMT) from *Candida albicans* as fungal targets together with dihydrofolate reductase (DHFR-B) and gyrase B (GyrB) from *Staphylococcus aureus* as bacterial targets.[29] Seven target proteins were selected for anticancer activity including DHFR-B, GyrB, DHFR-F, NMT, vascular endothelial growth factor receptor 2 (VEGFR-2), fibroblast growth factor receptor 1 (FGFR-1), and histone deacetylase 6 (HDAC6) whose dysregulation is linked to cancer cell proliferation. On the other hand, nine

Table 5 *In silico* molecular docking results of active compounds and standard drugs[a]

Compound	DHFR-B		GyrB		DHFR-F		NMT		VEGFR-2		FGFR-1		HDAC6	
	a	b	a	b	a	b	a	b	a	b	a	b	a	b
3k	−9.6	2 ASN18, THR121	−8.0	0	−8.5	2 ALA11, TRP27	−11.0	1 ASN392	−8.3	2 ARG1027	−9.7	0	−9.4	2 HIS192, HIS193
3l	−9.5	1 SER49	−7.9	0	−8.0	1 GLY23	−11.3	1 ASN392	−8.6	0	−9.3	0	−9.1	1 LYS330
4c	−10.0	1 SER49	−7.9	0	−8.4	0	−11.1	1 HIS227	−8.7	0	−9.6	0	−8.6	1 HIS232
4g	−10.0	1 ASN18	−8.1	0	−8.8	1 ALA11	−10.3	0	−8.7	2 ARG1027	−10.0	0	−9.5	2 HIS192, HIS193
4j	−9.9	1 ASN18	−8.0	0	−8.5	0	−10.6	0	−9.0	2 ARG1027	−9.5	1 ASP641	−9.4	2 HIS192, HIS193
Cipro	−9.1	1 SER49	−7.3	2 ASP81, SER55	—	—	—	—	—	—	—	—	—	—
Flu	—	—	—	—	−7.0	4 ALA115, GLU116, LYS57	−7.9	1 TYR225	—	—	—	—	—	—
PTX	−10.0	3 LEU20, SER49, THR121	−7.8	5 ASN54, ARG84, GLY85, THR173	−8.5	2 ARG28	−11.4	1 GLY213	−7.8	1 GLY1048	−10.5	3 ASN628, GLU486, THR658	−8.8	4 LYS330, SER150, VAL151

[a] The bacterial targets consist of DHFR-B – Dihydrofolate Reductase-Bacteria, GyrB – Gyrase B. The fungal targets consist of DHFR-F – Dihydrofolate Reductase-Fungi, NMT – *N*-myristoyl transferase, VEGFR-2 – vascular endothelial growth factor receptor 2, FGFR-1 – fibroblast growth factor receptor 1, HDAC6 – histone deacetylase 6. The cancer targets include all seven receptors. Cipro – Ciprofloxacin, Flu – Fluconazole, PTX – paclitaxel. *a* – affinity (kcal mol^{-1}), *b* – hydrogen bond (number, position).

poses of each potent compound were obtained by the docking simulations with each receptor and the pose with the highest affinity (model 0) was chosen to validate the activity.

Among all these seven proteins, two proteins (DHFR-B and NMT) as both antimicrobial and antitumor targets presented good binding affinity with a higher affinity than −9.5 kcal-mol^{-1}. On the other hand, two proteins (FGFR-1 and HDAC6) as antitumor targets presented good interactions with affinity in the range of −8.6 to −10.0 kcal mol^{-1}, while VEGFR-2 showed
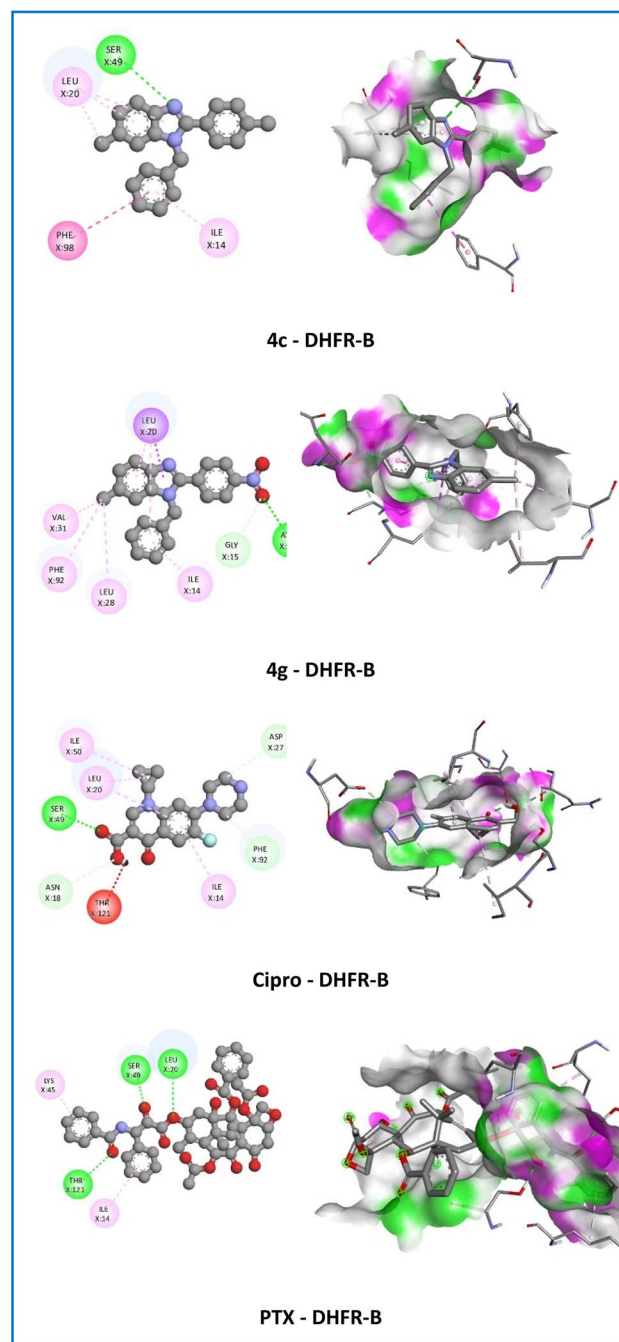
Fig. 5 2D and 3D representation of the interaction of the active compounds (**4c** and **4g**), ciprofloxacin (Cipro), and paclitaxel (PTX) with dihydrofolate reductase of bacteria (DHFR-B).

weaker interactions with affinity in the range of −8.3 to −9.0 kcal mol⁻¹ with active derivatives (Table 5). Here in our study, compound **4c** being the most potent antimicrobial and antitumor agent displayed the highest negative affinity of −10.0 kcal mol⁻¹ against DHFR-B, and the second negative affinity of −11.1 kcal mol⁻¹ against NMT from *S. aureus* which is comparable to Cipro (DHFR-B), Flu (NMT) and PTX (DHFR-B and NMT) with the affinity of −9.1, −7.9 and (−10.0 and −11.4) kcal mol⁻¹, respectively. Besides, this compound established one strong hydrogen bond with SER49 amino acid of DHFR-B with a bond length of 2.97 Å being similar to that of Cipro (2.20 Å) and PTX (1.87 Å). In addition, compound **4c** also established one strong hydrogen bond with HIS227 amino acid of NMT with a bond length of 2.21 Å which is comparable to Flu (TYR225, 2.36 Å), and PTX (GLY213, 2.23 Å). Although no hydrogen bond was established, compound **4c** showed a good affinity for FGFR1 of −9.6 kcal mol⁻¹ compared with PTX (−10.5 kcal mol⁻¹) which established three hydrogen bonds at ASN628, GLU486, and THR658 amino acids. Hence compound **4c** is considered the best dock conformation in antimicrobial and antitumor targets.

On the DHFR-B receptor, compound **3k** established two hydrogen bonds (2.30–2.67 Å) with the affinity (−9.6 kcal mol⁻¹) with ASN18, THR121 amino acids, but compounds **4g** and **4j** only established one hydrogen bond (2.35–2.58 Å) with the affinity (−9.9 to −10.0 kcal mol⁻¹) with ASN18 amino acid when compared with the standard drug Cipro (−9.1 kcal mol⁻¹) with one hydrogen bond (2.20 Å) with SER49 amino acid and PTX (−10.0 kcal mol⁻¹) with three hydrogen bonds (1.87–3.01 Å) with LEU20, SER49, THR121 amino acids (Fig. 5). However, compound **3l** (−9.5 kcal mol⁻¹) established one hydrogen bond (2.89 Å) with SER49 amino acid similar to **4c**, Cipro, and PTX. These results have demonstrated that compound **4c** is the most potential *in vitro* antibacterial and antitumor activities.

On the GyrB receptor, all active compounds showed good interactions with affinity in the range of −7.9 to −8.1 kcal mol⁻¹ compared with the standard drug Cipro (−7.3 kcal mol⁻¹) and PTX (−7.8 kcal mol⁻¹). Similarly, all active compounds also showed good interactions with affinity in the range of −8.0 to −8.8 kcal mol⁻¹ compared with the standard drug Flu (−7.0 kcal mol⁻¹) and PTX (−8.5 kcal mol⁻¹) on DHFR-F receptor. However, these compounds established fewer hydrogen bonds than the standard drugs.

On the NMT receptor, compounds **3k** and **3l** established one hydrogen bond (2.61–2.71 Å) with good affinity (−11.0 to −11.3 kcal mol⁻¹) with ASN392 amino acid compared with Flu (−7.9 kcal mol⁻¹), PTX (−11.4 kcal mol⁻¹), and **4c** (−11.1 kcal mol⁻¹) (Fig. 6). On the contrary, compounds **4g** and **4j** did not establish hydrogen bonds with affinity at −10.3 and −10.6 kcal mol⁻¹, respectively.

On the VEGFR-2 receptor, all active compounds showed stronger interactions with the affinity between −8.3 and −9.0 kcal mol⁻¹ compared with the reference drug PTX (−7.8 kcal mol⁻¹). Compounds **3k**, **4g**, and **4j** established one hydrogen bond (2.56–2.78 Å) with ARG1027 amino acid. Compounds **3l** and **4c** did not establish conventional hydrogen

bonds but established carbon-hydrogen bonds with ASP1046 amino acid with bond lengths in the range of 3.13 to 3.56 Å.

On the FGFR-1 receptor, all active compounds did not establish a hydrogen bond except for **4j** established one hydrogen bond (2.67 Å) with ASP641 amino acid. In addition, these compounds showed weaker interactions with the affinity between −9.3 and −10.0 kcal mol⁻¹ compared with the
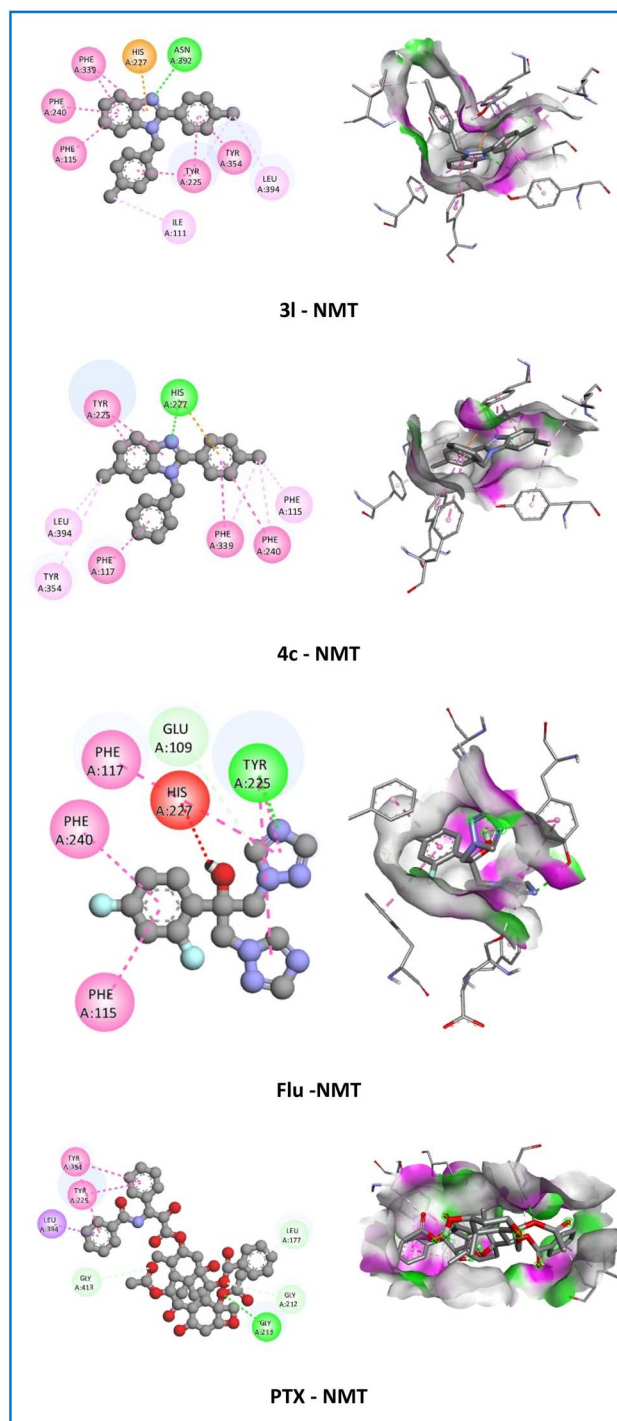

Fig. 6 2D and 3D representation of the interaction of the active compounds (**3l** and **4c**), fluconazole (Flu), and paclitaxel (PTX) with *N*-myristoyl transferase (NMT).

reference drug PTX (-10.5 kcal mol^{-1}). On the HDAC6 receptor, all active compounds showed stronger interactions with the affinity between -9.1 and -9.5 kcal mol^{-1} except for **4c** when compared with reference drug PTX (-8.8 kcal mol^{-1}). However, these compounds have formed fewer hydrogen bonds than PTX (Fig. 7). These results suggested that FGFR-1 and HDAC6 also are the most likely targets for the anticancer activity of these newly synthesized agents.

Among all the derivatives, compound **4c** showed hydrophobic interactions (π–π T-shaped, alkyl, π–alkyl) with PHE98, LEU20, and ILE14 with the crucial residue of the DHFR-B protein from *S. aureus* that resembles the co-crystallization ligand, Cipro, and PTX. As illustrated in Fig. 5, the 6-methyl (6-CH$_3$) group and 1*H*-benzimidazole nucleus of compound **4c** were engaged in the formation of alkyl and π–alkyl interactions with LEU20 amino acid with bond length in the range of 4.17–5.15 Å. Moreover, the *N*-benzyl group displayed π–π T-shaped

Table 6 The 50% inhibitory concentration (IC$_{50}$) of active compounds for *in vitro* DHFR inhibitory activity

Compound	DHFR inhibitory activities (IC$_{50}$, μM)
3k	12.32
3l	10.64
4c	**2.35**
4g	6.78
4j	8.01
Methotrexate	0.021

interaction with the crucial residue PHE98 of the target protein with a bond length of 5.47 Å and π–alkyl interaction with ILE14 amino acid with a bond length of 4.80 Å. On the other hand, compound **4c** also established electrostatic interaction (π–cation) and hydrophobic interactions (π–π stacked, π–π T-shaped, alkyl, π–alkyl) with the crucial residue of the NMT protein from *Candida albicans* that resembles the co-crystallization ligand, Flu, and PTX. The 6-methyl (6-CH$_3$) group showed alkyl and π–alkyl interactions with LEU394 and TYR354 amino acids with bond lengths in the range of 4.09–5.31 Å. In addition, the substituted part of compound **4c** moved inside the cavity where both the benzene ring of *N*-benzyl and 2-phenyl groups and the 1*H*-benzimidazole nucleus were observed to establish hydrophobic interactions (π–π stacked and π–π T-shaped) with TYR225, PHE240, PHE117, and PHE339 amino acids with a bond length of 3.82, 5.36, 5.03, and 5.04 Å, respectively. Besides, the 2-phenyl groups of the 1*H*-benzimidazole nucleus showed electrostatic interaction (π–cation) with HIS227 amino acid with a bond length of 4.24 Å. Especially, 4-chloro (4-Cl) of 2-phenyl ring displayed π–alkyl interaction with PHE115, PHE240, and PHE339 amino acids with a bond length of 3.55, 4.45, and 4.64 Å, respectively (Fig. 6). The resulting docking may therefore suggest that its potent antibacterial, antifungal, and antitumor activities are mediated *via* interaction with DHFR and NMT proteins.

As to the selectivity prediction, the binding affinity in the range of -9.4 to -10.6 kcal mol^{-1} of compounds **4g** and **4j** are essentially similar on the DHFR-B, NMT, FGFR-1, and HDAC6 receptors. Compounds **3k** and **3l** showed similar affinity (-9.1 to -9.7 kcal mol^{-1}) on the DHFR-B, FGFR-1, and HDAC6 receptors. However, compounds **3k**, **3l**, and **4c** are predicted to be selective on the NMT receptor as having high affinity in the range of -11.0 to -11.3 kcal mol^{-1}. Moreover, compound **4c** also exhibited higher selectivity on the DHFR receptor than other potential compounds due to the difference in the range of -1.3 to -2.1 kcal mol^{-1} compared with GyrB, DHFR-F, VEGFR-2, and HDAC6 receptors.

2.6. *In vitro* DHFR inhibitory activity

The results of *in silico* molecular docking studies have predicted that DHFR is a potential receptor to explain the mechanism of antimicrobial and anticancer activities for the active derivatives. So, these compounds were tested for their ability to inhibit
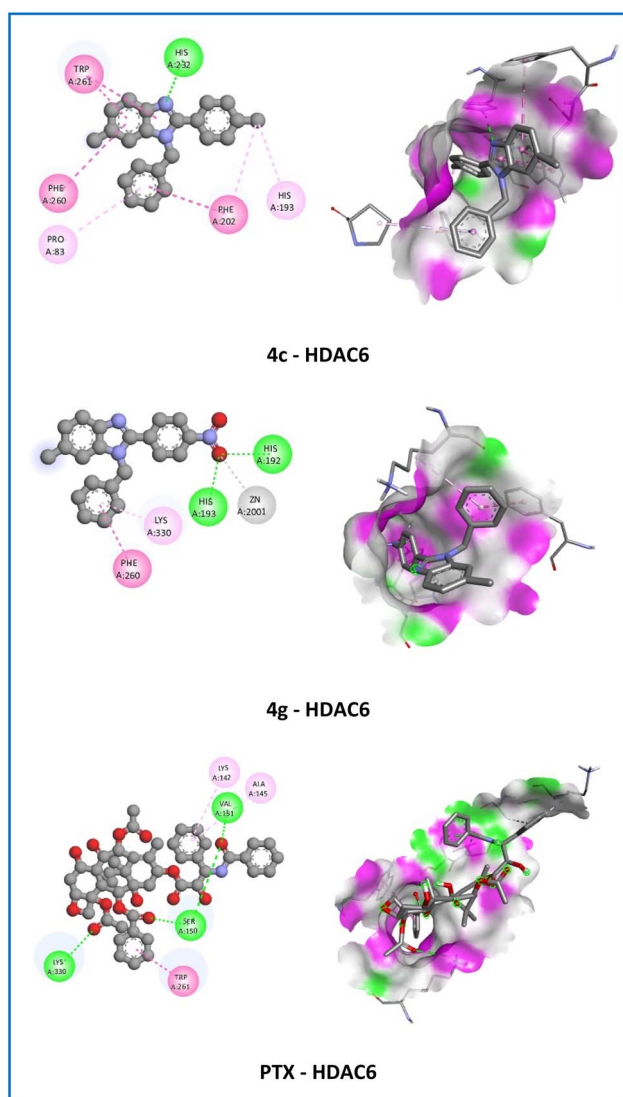
Fig. 7 2D and 3D representation of the interaction of the active compounds (**4c** and **4g**), and paclitaxel (PTX) with histone deacetylase 6 (HDAC6).

human DHFR and their potencies (IC$_{50}$ values) were measured *in vitro*. DHFR inhibition assay kit, involving the DHFR-mediated conversion of dihydrofolate to tetrahydrofolate in the presence of NADPH (reduced nicotinamide adenine dinucleotide phosphate) has been used to investigate the inhibition of DHFR of active compounds **3k**, **3l**, **4c**, **4g**, and **4j**. It has been observed that compound **4c** showed the best activity at a low µM concentration of 2.35 µM (Table 6). In addition, compounds **3k**, **3l**, **4g**, and **4j** showed good inhibitory activity towards DHFR enzyme immunoassay with IC$_{50}$ in the range of 6.78–12.32 µM. On the other hand, benzimidazole derivatives, for example, quinazolinone-benzimidazole and triazine-benzimidazole hybrids have also been reported to strongly inhibit DHFR.[30,48] Therefore, the results suggest that DHFR is a target for compound **4c**'s antimicrobial and anticancer activities as shown by both *in silico* and *in vitro* studies.

3. Conclusion

In summary, starting from 1,2phenylenediamine and 4-Me-1,2-phenylenediamine, forty-six 2,6-disubstituted 1*H*-benzimidazole and twenty-three *N*,2,6-trisubstituted 1*H*-benzimidazole derivatives including sixteen new compounds have been designed, synthesized, and evaluated for their antimicrobial and anticancer activities. The microwave-assisted method has contributed to a significant reduction in reaction time and a significant increase in product yield. In addition, the values of the MIC against microorganisms showed that some compounds have significant inhibitory effects, especially compounds **3k**, **3l**, **4c**, **4g**, and **4j** are potent for antibacterial activity against Gram-positive and Gram-negative bacteria compared with standard drug Cipro while compounds **3k**, **3l**, and **4c** are potent for antifungal activity compared with standard drug Flu. In particular, these compounds also exhibited potent anticancer activity with IC$_{50}$ < 10 µM against all tested cell lines (HepG2, MDA-MB-231, MCF7, RMS, and C26) compared with the reference drug PTX. From the structure–activity relationship, the presence of the *N*-benzyl group and the 4-chloro/4-nitro group in the aromatic ring at position 2 of the 1*H*-benzimidazole scaffold is more desirable for enhanced antibacterial activity as well as antitumor activity in **3f**, **3l**, **3k**, **4c**, and **4j**, and antifungal activity in **3l** and **4c**. Molecular docking predicted that DHFR (dihydrofolate reductase) protein from *S. aureus* and NMT (*N*-myristoyl transferase) protein from *C. albicans* are the most suitable targets for the antimicrobial and anticancer activities. Compound **4c** being the most potent antimicrobial and anticancer displayed a good affinity of −11.1 kcal mol^{-1} with the NMT enzyme from *C. albicans* and showed a good affinity of −10.0 kcal mol^{-1} with the crucial residue of the DHFR-B protein from *S. aureus* as well as showed electrostatic and hydrophobic interactions that resemble the co-crystallization ligand and reference drugs. Moreover, compound **4c** showed good activity at a low µM concentration of 2.35 µM. Computational ADMET profiling for the five most active compounds in comparison to ciprofloxacin, fluconazole, and paclitaxel as reference drugs suggests that our derivatives have good ADMET profiles. Moreover, all compounds show physical–chemical properties of

fragment and lead-like compounds which are of great interest for further drug development. This work paved the way for the synthesis of more potent antimicrobial and anticancer benzimidazole derivatives.

4. Experimental section

4.1. Materials

All chemicals and solvents were of analytical grade and obtained from Merck, Germany. The reactions were monitored by thin-layer chromatography (TLC, E-Merck Kieselgel 60 F$_{254}$). The column chromatography was carried out with the indicated solvents using silica gel (particle size 0.040–0.063 mm) from Merck (Germany). The microwave-assisted reactions were performed by the microwave synthesizer (CEM Discover, USA) with continuous stirring and controlled temperature. Melting points (mp, °C) of all compounds were determined in an open capillary using a Gallenkamp melting point apparatus without any correction. The infrared (IR) spectra were recorded using a Shimadzu FT-IR (IRAffinity-1S) spectrometer. An Agilent Technology LC-mass spectrometer with ESI ionization (1100 series LC/MSD Trap) was used to record the mass spectra (MS). A Bruker Avance 500 (^{1}H, 500 MHz; ^{13}C, 125 MHz) NMR spectrometer was used to record the ^{1}H NMR and ^{13}C NMR spectra at ambient temperature using DMSO-d$_6$ as solvent. Chemical shifts are reported in parts per million (ppm) relative to the residual solvent peak as follows: DMSO-d$_6$ = 2.50 ppm (^{1}H NMR) and DMSO-d$_6$ = 40.00 ppm (^{13}C NMR). The Multiskan microplate reader was used to measure optical density (OD) at 570 nm.

4.2. Experimental procedures

4.2.1 General procedure for the preparation of 2,6-disubstituted 1*H*-benzimidazole derivatives (1a–1w and 2a–w)

4.2.1.1 Refluxing method. A mixture of benzene-1,2-diamine or 4-methylbenzene-1,2-diamine (5 mmol), the substituted aromatic aldehydes (5 mmol), and Na$_2$S$_2$O$_5$ (20 mmol) in a mixture of EtOH : H$_2$O (30 mL, 9 : 1, v/v) was refluxed for 6–12 h at 80 °C. After cooling down, the mixture was poured into cooled water and filtered off in a Büchner funnel. The resulting solid was purified by silica gel column chromatography using hexane/ethyl acetate as eluent. Yields: 75–93%.

4.2.1.2 Microwave-assisted method. A mixture of benzene-1,2-diamine or 4-methylbenzene-1,2-diamine (5 mmol), the substituted aromatic aldehydes (5 mmol), Na$_2$S$_2$O$_5$ (20 mmol) in a mixture of EtOH : H$_2$O (10 mL, 9 : 1, v/v) was placed in a microwave oven and irradiated at a power of 300 W for 10–15 min at 80 °C. After cooling down, the mixture was poured into cooled water and filtered off in a Büchner funnel. The resulting solid was purified by silica gel column chromatography using hexane/ethyl acetate as eluent. Yields: 90–99%.

2-(2-Chlorophenyl)-1H-benzimidazole (1a): yellow solid, mp 228–229 °C. ^{1}H NMR (500 MHz, DMSO-d$_6$, δ ppm): 12.70 (1H, s, –NH–), 7.90 (1H, dd, *J* = 7.5, 2.0 Hz, H$_{Ar}$), 7.66–7.61 (3H, m, H$_{Ar}$), 7.56–7.50 (2H, m, H$_{Ar}$), 7.24 (2H, m, H$_{Ar}$). ^{13}C NMR (125 MHz, DMSO-d$_6$, δ ppm): 149.0, 132.0, 131.6, 131.1, 130.7, 130.3, 129.9,

127.4, 122.2. LC-MS (m/z) $[M - H]^-$ calcd for $C_{13}H_8ClN_2$ 227.0381, found 227.0399; $[M + H]^+$ calcd for $C_{13}H_{10}ClN_2$ 229.0527, found 229.0462.

2-(4-Chlorophenyl)-1H-benzimidazole (1b): yellow solid, mp 290–291 °C. ^{1}H NMR (500 MHz, DMSO-d_6, δ ppm): 8.19 (2H, d, J = 8.5 Hz, H_{Ar}), 7.63–7.60 (4H, m, H_{Ar}), 7.22 (2H, d, J = 8.5 Hz, H_{Ar}). ^{13}C NMR (125 MHz, DMSO-d_6, δ ppm): 150.2, 134.6, 131.2, 130.8, 129.1, 129.0, 128.98, 128.8, 128.78, 128.2, 128.0, 122.4. LC-MS (m/z) $[M - H]^-$ calcd for $C_{13}H_8ClN_2$ 227.0381, found 227.0389; $[M + H]^+$ calcd for $C_{13}H_{10}ClN_2$ 229.0527, found 229.0636.

2-(2,4-Dichlorophenyl)-1H-benzimidazole (1c): white solid, mp 232–233 °C. ^{1}H NMR (500 MHz, DMSO-d_6, δ ppm): 12.77 (1H, s, –NH–), 7.94 (1H, d, J = 8.5 Hz, H_{Ar}), 7.85 (1H, d, J = 2.0 Hz, H_{Ar}), 7.70 (1H, s, H_{Ar}), 7.63–7.58 (2H, m, H_{Ar}), 7.25 (2H, s, H_{Ar}). ^{13}C NMR (125 MHz, DMSO-d_6, δ ppm): 148.1, 143.1, 135.0, 134.6, 133.2, 132.6, 129.9, 128.9, 127.7, 122.9, 121.8, 119.2, 111.8. LC-MS (m/z) $[M - H]^-$ calcd for $C_{13}H_7Cl_2N_2$ 260.9992, found 260.9952; $[M + H]^+$ calcd for $C_{13}H_9Cl_2N_2$ 263.0137, found 262.9776.

2-(3,4-Dichlorophenyl)-1H-benzimidazole (1d): white solid, mp 237–238 °C. ^{1}H NMR (500 MHz, DMSO-d_6, δ ppm): 13.07 (1H, s, –NH–), 8.39 (1H, d, J = 1.0 Hz, H_{Ar}), 8.15 (1H, dd, J = 8.0, 1.0 Hz, H_{Ar}), 7.83 (1H, d, J = 8.5 Hz, H_{Ar}), 7.67–7.57 (2H, m, H_{Ar}), 7.24 (2H, s, H_{Ar}). ^{13}C NMR (125 MHz, DMSO-d_6, δ ppm): 148.8, 132.2, 131.8, 131.3, 131.0, 130.9, 130.7, 127.9, 126.4, 123.1, 122.1, 119.0, 111.5. LC-MS (m/z) $[M - H]^-$ calcd for $C_{13}H_7Cl_2N_2$ 260.9992, found 260.9905; $[M + H]^+$ calcd for $C_{13}H_9Cl_2N_2$ 263.0137, found 262.9993.

2-(2-Chloro-6-fluorophenyl)-1H-benzimidazole (1e): white solid, mp 225–226 °C. ^{1}H NMR (500 MHz, DMSO-d_6, δ ppm): 12.91 (1H, s, –NH–), 7.80–7.50 (4H, m, H_{Ar}), 7.46 (1H, d, J = 8.0 Hz, H_{Ar}), 7.26 (2H, s, H_{Ar}). ^{13}C NMR (125 MHz, DMSO-d_6, δ ppm): 161.7, 159.7, 143.5, 134.30, 134.27, 132.65, 132.57, 125.86, 125.84, 122.78, 121.6, 119.90, 119.74, 119.27, 115.0, 114.82, 111.6. LC-MS (m/z) $[M - H]^-$ calcd for $C_{13}H_7ClFN_2$ 245.0287, found 245.0257; $[M + H]^+$ calcd for $C_{13}H_9ClFN_2$ 247.0433, found 247.0338.

2-(3,4-Dimethoxyphenyl)-1H-benzimidazole (1f): yellow solid, mp 232–233 °C. ^{1}H NMR (500 MHz, DMSO-d_6, δ ppm): 12.74 (1H, s, –NH–), 7.78 (1H, s, H_{Ar}), 7.75 (1H, d, J = 8.0 Hz, H_{Ar}), 7.62–7.50 (2H, m, H_{Ar}), 7.18–7.12 (3H, m, H_{Ar}), 3.88 (3H, s, –OCH$_3$), 3.84 (3H, s, –OCH$_3$). ^{13}C NMR (125 MHz, DMSO-d_6, δ ppm): 151.4, 150.3, 148.9, 143.9, 134.9, 122.7, 122.1, 121.5, 119.3, 118.5, 118.3, 111.9, 111.7, 111.0, 109.8, 55.6. LC-MS (m/z) $[M - H]^-$ calcd for $C_{15}H_{13}N_2O_2$ 253.0983, found 254.1055; $[M + H]^+$ calcd for $C_{15}H_{15}N_2O_2$ 255.1128, found 255.0914.

2-(4-Ethoxyphenyl)-1H-benzimidazole (1g): white solid, mp 259–261 °C. ^{1}H NMR (500 MHz, DMSO-d_6, δ ppm): 12.71 (1H, s, –NH–), 8.10 (2H, d, J = 8.5 Hz, H_{Ar}), 7.56–7.54 (2H, m, H_{Ar}), 7.17–7.16 (2H, m, H_{Ar}), 7.09 (2H, d, J = 9.0 Hz, H_{Ar}), 4.11 (2H, q, J = 7.0 Hz, –CH$_2$–), 1.36 (3H, t, J = 7.0 Hz, –CH$_3$). ^{13}C NMR (125 MHz, DMSO-d_6, δ ppm): 159.8, 151.3, 128.0, 122.5, 121.7, 114.7, 63.2, 14.6. LC-MS (m/z) $[M - H]^-$ calcd for $C_{15}H_{13}N_2O$ 237.1033, found 237.0655; $[M + H]^+$ calcd for $C_{15}H_{15}N_2O$ 239.1179, found 239.0670.

4-(1H-Benzimidazol-2-yl)-2-ethoxyphenol (1h): yellow solid, mp 193–194 °C. ^{1}H NMR (500 MHz, DMSO-d_6, δ ppm): 12.62 (1H, s, –NH–), 9.44 (1H, s, –OH), 7.73 (1H, d, J = 2.0 Hz, H_{Ar}), 7.61 (1H, dd, J = 8.5, 2.0 Hz, H_{Ar}), 7.53 (2H, s, H_{Ar}), 7.21–7.14 (2H, m, H_{Ar}), 6.93 (1H, d, J = 8.5 Hz, H_{Ar}), 4.14 (2H, q, J = 7.0 Hz, –CH$_2$–), 1.40 (3H, t, J = 7.0 Hz, –CH$_3$). ^{13}C NMR (125 MHz, DMSO-d_6, δ ppm): 151.8, 148.7, 147.0, 121.4, 119.7, 115.8, 111.6, 64.0, 14.7. LC-MS (m/z) $[M - H]^-$ calcd for $C_{15}H_{13}N_2O_2$ 253.0983, found 253.1013; $[M + H]^+$ calcd for $C_{15}H_{15}N_2O_2$ 255.1128, found 255.1011.

2-(4-Fluorophenyl)-1H-benzimidazole (1i): yellow solid, mp 255–256 °C. ^{1}H NMR (500 MHz, DMSO-d_6, δ ppm): 12.89 (1H, s, –NH–), 8.23–8.20 (2H, m, H_{Ar}), 7.66 (1H, d, J = 7.5 Hz, H_{Ar}), 7.53 (1H, d, J = 7.5 Hz, H_{Ar}), 7.40 (2H, t, J = 9.0 Hz, H_{Ar}), 7.25–7.17 (2H, m, H_{Ar}). ^{13}C NMR (125 MHz, DMSO-d_6, δ ppm): 164.0, 162.1, 150.4, 143.7, 135.0, 128.72, 128.65, 126.78, 126.76, 122.5, 121.7, 118.8, 116.1, 115.9, 111.3. LC-MS (m/z) $[M - H]^-$ calcd for $C_{13}H_8FN_2$ 211.0677, found 211.0679; $[M + H]^+$ calcd for $C_{13}H_{10}FN_2$ 213.0823, found 213.0708.

2-(1H-Benzimidazol-2-yl)phenol (1j): white solid, mp 246–248 °C. ^{1}H NMR (500 MHz, DMSO-d_6, δ ppm): 13.19 (1H, s, –NH–), 7.85 (1H, d, J = 7.0 Hz, H_{Ar}), 7.64 (1H, d, J = 7.5 Hz, H_{Ar}), 7.48 (1H, d, J = 7.5 Hz, H_{Ar}), 7.30–7.16 (4H, m, H_{Ar}), 7.02 (1H, d, J = 7.5 Hz, H_{Ar}). ^{13}C NMR (125 MHz, DMSO-d_6, δ ppm): 158.5, 151.7, 141.5, 133.6, 131.4, 129.6, 124.2, 119.2, 117.3, 111.5. LC-MS (m/z) $[M - H]^-$ calcd for $C_{13}H_9N_2O$ 209.0720, found 209.0822; $[M + H]^+$ calcd for $C_{13}H_{11}N_2O$ 211.0866, found 211.0854.

2-(1H-Benzimidazol-2-yl)-4-bromophenol (1k): brown solid, mp 280–282 °C. ^{1}H NMR (500 MHz, DMSO-d_6, δ ppm): 13.27 (1H, s, –NH–), 8.29 (1H, d, J = 2.0 Hz, H_{Ar}), 7.70–7.66 (2H, m, H_{Ar}), 7.52 (1H, dd, J = 9.0, 2.0 Hz, H_{Ar}), 7.32–7.30 (2H, m, H_{Ar}), 7.02 (1H, d, J = 9.0 Hz, H_{Ar}). ^{13}C NMR (125 MHz, DMSO-d_6, δ ppm): 157.1, 150.2, 134.0, 128.4, 122.7, 119.4, 114.6, 111.7, 110.1. LC-MS (m/z) $[M - H]^-$ calcd for $C_{13}H_8BrN_2O$ 286.9825, found 287.0522; $[M + H]^+$ calcd for $C_{13}H_{10}BrN_2O$ 288.9971, found 289.0718.

3-(1H-Benzimidazol-2-yl)phenol (1l): yellow solid, mp 261–263 °C. ^{1}H NMR (500 MHz, DMSO-d_6, δ ppm): 12.84 (1H, s, –NH–), 9.78 (1H, s, –OH), 7.66–7.51 (4H, m, H_{Ar}), 7.34 (1H, t, J = 8.0 Hz, H_{Ar}), 7.27–7.08 (2H, m, H_{Ar}), 6.91 (1H, d, J = 8.0 Hz, H_{Ar}). ^{13}C NMR (125 MHz, DMSO-d_6, δ ppm): 157.8, 151.4, 143.8, 135.0, 131.4, 130.1, 129.9, 122.5, 121.7, 118.9, 117.3, 117.0, 113.4, 111.3. LC-MS (m/z) $[M - H]^-$ calcd for $C_{13}H_9N_2O$ 209.0720, found 209.0724; $[M + H]^+$ calcd for $C_{13}H_{11}N_2O$ 211.0866, found 211.0859.

5-(1H-Benzimidazol-2-yl)-2-methoxyphenol (1m): yellow solid, mp 238–240 °C. ^{1}H NMR (500 MHz, DMSO-d_6, δ ppm): 12.68 (1H, s, –NH–), 9.32 (1H, s, –OH), 7.67 (1H, s, H_{Ar}), 7.62 (1H, d, J = 8.5 Hz, H_{Ar}), 7.56–7.54 (2H, m, H_{Ar}), 7.17–7.15 (2H, m, H_{Ar}), 7.09 (1H, d, J = 8.5 Hz, H_{Ar}), 3.85 (3H, s, –OCH$_3$). ^{13}C NMR (125 MHz, DMSO-d_6, δ ppm): 151.6, 149.4, 146.7, 123.0, 121.7, 118.0, 113.8, 112.2, 55.7. LC-MS (m/z) $[M - H]^-$ calcd for $C_{14}H_{11}N_2O_2$ 239.0826, found 239.0592; $[M + H]^+$ calcd for $C_{14}H_{13}N_2O_2$ 241.0972, found 241.0712.

2-(3-Methoxyphenyl)-1H-benzimidazole (1n): yellow solid, mp 207–208 °C. ^{1}H NMR (500 MHz, DMSO-d_6, δ ppm): 12.87 (1H, s, –NH–), 7.76 (2H, d, J = 7.0 Hz, H_{Ar}), 7.67 (1H, d, J = 8.0 Hz, H_{Ar}), 7.53 (1H, d, J = 7.5 Hz, H_{Ar}), 7.46 (1H, t, J = 8.0 Hz, H_{Ar}), 7.24–7.17 (2H, m, H_{Ar}), 7.06 (1H, dd, J = 7.0, 2.5 Hz, H_{Ar}), 3.87 (3H, s,

–OCH$_3$). ^{13}C NMR (125 MHz, DMSO-d$_6$, δ ppm): 159.6, 151.0, 143.7, 134.9, 131.4, 130.0, 122.5, 121.6, 118.8, 118.7, 115.8, 111.4, 111.3, 55.3. LC-MS (m/z) [M – H]$^-$ calcd for C$_{14}$H$_{11}$N$_2$O 223.0877, found 223.0852; [M + H]$^+$ calcd for C$_{14}$H$_{13}$N$_2$O 225.1022, found 225.0894.

2-(4-(Methylthio)phenyl)-1H-benzimidazole (1o): brown solid, mp 101–102 °C. ^{1}H NMR (500 MHz, DMSO-d$_6$, δ ppm): 12.81 (1H, s, –NH–), 8.05 (2H, d, J = 8.5 Hz, H$_{Ar}$), 7.66 (1H, d, J = 7.5 Hz, H$_{Ar}$), 7.50 (1H, d, J = 7.5 Hz, H$_{Ar}$), 7.43 (2H, d, J = 8.5 Hz, H$_{Ar}$), 7.23–7.15 (2H, m, H$_{Ar}$), 2.57 (3H, s, –SCH$_3$). ^{13}C NMR (125 MHz, DMSO-d$_6$, δ ppm): 151.2, 141.5, 131.8, 127.4, 126.9, 126.0, 124.1, 14.9. LC-MS (m/z) [M – H]$^-$ calcd for C$_{14}$H$_{11}$N$_2$S 239.0648, found 239.0601; [M + H]$^+$ calcd for C$_{14}$H$_{13}$N$_2$S 241.0794, found 241.0801.

2-(3-Nitrophenyl)-1H-benzimidazole (1p): yellow solid, mp 205–207 °C. ^{1}H NMR (500 MHz, DMSO-d$_6$, δ ppm): 13.26 (1H, s, –NH–), 8.99 (1H, s, H$_{Ar}$), 8.59 (1H, d, J = 8.0 Hz, H$_{Ar}$), 8.28 (1H, d, J = 8.0 Hz, H$_{Ar}$), 7.81 (1H, t, J = 8.0 Hz, H$_{Ar}$), 7.64 (2H, s, H$_{Ar}$), 7.25–7.23 (2H, m, H$_{Ar}$). ^{13}C NMR (125 MHz, DMSO-d$_6$, δ ppm): 149.0, 148.3, 132.4, 131.7, 130.6, 124.1, 122.6, 120.8. LC-MS (m/z) [M – H]$^-$ calcd for C$_{13}$H$_8$N$_3$O$_2$ 238.0622, found 238.0592; [M + H]$^+$ calcd for C$_{13}$H$_{10}$N$_3$O$_2$ 240.0768, found 240.0730.

2-(4-Nitrophenyl)-1H-benzimidazole (1q): yellow solid, mp 319–320 °C. ^{1}H NMR (500 MHz, DMSO-d$_6$, δ ppm): 13.29 (1H, s, –NH–), 8.43–8.39 (4H, m, H$_{Ar}$), 7.70–7.63 (2H, m, H$_{Ar}$), 7.27 (2H, s, H$_{Ar}$). ^{13}C NMR (125 MHz, DMSO-d$_6$, δ ppm): 149.0, 147.8, 136.0, 127.4, 124.3, 123.5, 119.5, 111.8. LC-MS (m/z) [M – H]$^-$ calcd for C$_{13}$H$_8$N$_3$O$_2$ 238.0622, found 238.0647; [M + H]$^+$ calcd for C$_{13}$H$_{10}$N$_3$O$_2$ 240.0768, found 240.0723.

4-(1H-Benzimidazol-2-yl)-N,N-dimethylaniline (1r): yellow solid, mp 287–289 °C. ^{1}H NMR (500 MHz, DMSO-d$_6$, δ ppm): 12.33 (1H, s, –NH–), 7.96 (2H, d, J = 8.5 Hz, H$_{Ar}$), 7.67 (1H, d, J = 7.5 Hz, H$_{Ar}$), 7.53 (1H, d, J = 7.5 Hz, H$_{Ar}$), 7.22–7.11 (2H, m, H$_{Ar}$), 6.81 (2H, d, J = 9.0 Hz, H$_{Ar}$), 2.98 (6H, s, –N(CH$_3$)$_2$). ^{13}C NMR (125 MHz, DMSO-d$_6$, δ ppm): 151.4, 127.5, 122.8, 117.7, 111.6, 40.2. LC-MS (m/z) [M + H]$^+$ calcd for C$_{15}$H$_{16}$N$_3$ 238.1339, found 238.1368.

2-(Anthracen-9-yl)-1H-benzimidazole (1s): yellow solid, mp 313–314 °C. ^{1}H NMR (500 MHz, DMSO-d$_6$, δ ppm): 13.01 (1H, s, –NH–), 8.85 (1H, s, H$_{Ar}$), 8.22 (2H, d, J = 8.5 Hz, H$_{Ar}$), 7.60 (4H, d, J = 8.5 Hz, H$_{Ar}$), 7.60–7.50 (4H, m, H$_{Ar}$), 7.32 (2H, m, H$_{Ar}$). ^{13}C NMR (125 MHz, DMSO-d$_6$, δ ppm): 149.5, 130.6, 130.5, 128.8, 128.4, 126.8, 125.8, 125.6, 125.5, 122.0. LC-MS (m/z) [M – H]$^-$ calcd for C$_{21}$H$_{13}$N$_2$ 293.1084, found 293.1032; [M + H]$^+$ calcd for C$_{21}$H$_{15}$N$_2$ 295.1230, found 295.1241.

2-(Benzo[d][1,3]dioxol-5-yl)-1H-benzimidazole (1t): yellow solid, mp 251–252 °C. ^{1}H NMR (500 MHz, DMSO-d$_6$, δ ppm): 12.72 (1H, s, –NH–), 7.72 (1H, dd, J = 8.0, 2.0 Hz, H$_{Ar}$), 7.68 (1H, d, J = 1.5 Hz, H$_{Ar}$), 7.62 (1H, d, J = 7.5 Hz, H$_{Ar}$), 7.49 (1H, d, J = 7.0 Hz, H$_{Ar}$), 7.18 (2H, t, J = 7.5 Hz, H$_{Ar}$), 7.09 (1H, d, J = 8.0 Hz, H$_{Ar}$), 6.12 (2H, s, –CH$_2$–). ^{13}C NMR (125 MHz, DMSO-d$_6$, δ ppm): 151.1, 148.7, 147.9, 143.7, 134.9, 124.2, 122.2, 121.5, 120.9, 118.6, 111.1, 108.7, 106.5, 101.6. LC-MS (m/z) [M – H]$^-$ calcd for C$_{14}$H$_9$N$_2$O$_2$ 237.0670, found 237.0655; [M + H]$^+$ calcd for C$_{14}$H$_{11}$N$_2$O$_2$ 239.0815, found 239.0670.

2-(Furan-2-yl)-1H-benzimidazole (1u): brown solid, mp 280–282 °C. ^{1}H NMR (500 MHz, DMSO-d$_6$, δ ppm): 12.74 (1H, s, –NH–), 7.92 (1H, d, J = 4.0 Hz, H$_{Ar}$), 7.69 (1H, d, J = 7.5 Hz, H$_{Ar}$), 7.55 (1H, d, J = 7.5 Hz, H$_{Ar}$), 7.23–7.19 (2H, m, H$_{Ar}$), 7.14 (1H, d, J = 4.0 Hz, H$_{Ar}$), 6.72 (1H, dd, J = 4.0, 2.0 Hz, H$_{Ar}$). ^{13}C NMR (125 MHz, DMSO-d$_6$, δ ppm): 146.8, 144.7, 143.5, 142.3, 132.8, 123.6, 118.5, 112.8, 110.4. LC-MS (m/z) [M – H]$^-$ calcd for C$_{11}$H$_7$N$_2$O 183.0564, found 183.0571; [M + H]$^+$ calcd for C$_{11}$H$_9$N$_2$O 185.0709, found 185.0802.

2-(Pyridin-3-yl)-1H-benzimidazole (1v): yellow solid, mp 240–241 °C. ^{1}H NMR (500 MHz, DMSO-d$_6$, δ ppm): 12.95 (1H, s, –NH–), 9.33 (1H, d, J = 1.5 Hz, H$_{Ar}$), 8.69 (1H, d, J = 3.5 Hz, H$_{Ar}$), 8.51 (1H, d, J = 8.0 Hz, H$_{Ar}$), 7.71 (1H, d, J = 7.5 Hz, H$_{Ar}$), 7.60 (1H, d, J = 7.5 Hz, H$_{Ar}$), 7.37 (1H, s, H$_{Ar}$), 7.25–7.20 (2H, m, H$_{Ar}$). ^{13}C NMR (125 MHz, DMSO-d$_6$, δ ppm): 150.5, 148.6, 147.5, 133.5, 126.2, 124.3, 123.8, 118.9, 111.2. LC-MS (m/z) [M – H]$^-$ calcd for C$_{12}$H$_8$N$_3$ 194.0724, found 194.0732.

2-(Pyridin-4-yl)-1H-benzimidazole (1w): yellow solid, mp 216–217 °C. ^{1}H NMR (500 MHz, DMSO-d$_6$, δ ppm): 13.26 (1H, s, –NH–), 8.76 (2H, dd, J = 4.5, 1.5 Hz, H$_{Ar}$), 8.10 (2H, dd, J = 4.5, 1.5 Hz, H$_{Ar}$), 7.74 (1H, d, J = 8.0 Hz, H$_{Ar}$), 7.60 (1H, d, J = 8.0 Hz, H$_{Ar}$), 7.31–7.23 (2H, m, H$_{Ar}$). ^{13}C NMR (125 MHz, DMSO-d$_6$, δ ppm): 150.5, 148.8, 143.6, 137.1, 135.0, 123.6, 122.3, 120.3, 119.5, 111.8. LC-MS (m/z) [M – H]$^-$ calcd for C$_{12}$H$_8$N$_3$ 194.0724, found 194.0728.

2-(2-Chlorophenyl)-6-methyl-1H-benzimidazole (2a): brown solid, mp 140–141 °C. ^{1}H NMR (500 MHz, DMSO-d$_6$, δ ppm): 12.55 (1H, s, –NH–), 7.89 (1H, d, J = 5.5 Hz, H$_{Ar}$), 7.65 (1H, dd, J = 9.0, 1.5 Hz, H$_{Ar}$), 7.58–7.45 (3H, m, H$_{Ar}$), 7.35 (1H, s, H$_{Ar}$), 7.10–7.04 (1H, m, H$_{Ar}$), 2.45 (3H, s, –CH$_3$). ^{13}C NMR (125 MHz, DMSO-d$_6$, δ ppm): 141.4, 134.9, 132.0, 131.6, 131.1, 130.3, 130.0, 127.4, 124.2, 123.3, 118.74, 118.65, 111.4, 111.2, 21.3. LC-MS (m/z) [M – H]$^-$ calcd for C$_{14}$H$_{10}$ClN$_2$ 241.0538, found 241.0005; [M + H]$^+$ calcd for C$_{14}$H$_{12}$ClN$_2$ 243.0684, found 243.0598.

2-(4-Chlorophenyl)-6-methyl-1H-benzimidazole (2b): brown solid, mp 216–217 °C. ^{1}H NMR (500 MHz, DMSO-d$_6$, δ ppm): 12.81 (1H, s, –NH–), 8.15 (2H, d, J = 8.5 Hz, H$_{Ar}$), 7.62 (2H, d, J = 8.5 Hz, H$_{Ar}$), 7.48–7.32 (2H, m, H$_{Ar}$), 7.03 (1H, d, J = 8.0 Hz, H$_{Ar}$), 2.50 (3H, s, –CH$_3$). ^{13}C NMR (125 MHz, DMSO-d$_6$, δ ppm): 134.2, 129.2, 129.0, 128.0, 21.3. LC-MS (m/z) [M + H]$^+$ calcd for C$_{14}$H$_{12}$ClN$_2$ 243.0684, found 243.0676.

2-(2,4-Dichlorophenyl)-6-methyl-1H-benzimidazole (2c): white solid, mp 142–144 °C. ^{1}H NMR (500 MHz, DMSO-d$_6$, δ ppm): 12.78 (1H, s, –NH–), 7.93 (1H, d, J = 8.5 Hz, H$_{Ar}$), 7.82 (1H, d, J = 2.0 Hz, H$_{Ar}$), 7.60 (1H, dd, J = 8.5, 2.0 Hz, H$_{Ar}$), 7.52 (1H, d, J = 8.0 Hz, H$_{Ar}$), 7.42 (1H, s, H$_{Ar}$), 7.08 (1H, d, J = 8.0 Hz, H$_{Ar}$), 2.44 (3H, s, –CH$_3$). ^{13}C NMR (125 MHz, DMSO-d$_6$, δ ppm): 147.6, 134.9, 133.2, 132.5, 131.7, 129.8, 128.8, 127.7, 123.9, 21.3. LC-MS (m/z) [M – H]$^-$ calcd for C$_{14}$H$_9$Cl$_2$N$_2$ 275.0148, found 275.0288; [M + H]$^+$ calcd for C$_{14}$H$_{11}$Cl$_2$N$_2$ 277.0294, found 277.1055.

2-(3,4-Dichlorophenyl)-6-methyl-1H-benzimidazole (2d): white solid, mp 134–136 °C. ^{1}H NMR (500 MHz, DMSO-d$_6$, δ ppm): 12.76 (1H, s, –NH–), 8.36 (1H, d, J = 1.5 Hz, H$_{Ar}$), 8.11 (1H, dd, J = 8.5, 1.5 Hz, H$_{Ar}$), 7.79 (1H, d, J = 8.5 Hz, H$_{Ar}$), 7.49 (1H, d, J = 8.5 Hz, H$_{Ar}$), 7.39 (1H, s, H$_{Ar}$), 7.05 (1H, d, J = 8.0 Hz, H$_{Ar}$), 2.42 (3H, s, –CH$_3$). ^{13}C NMR (125 MHz, DMSO-d$_6$, δ ppm): 148.5, 132.1, 132.0, 131.8, 131.2, 131.0, 130.9, 130.8, 129.3, 127.8, 126.3, 124.1, 21.3. LC-MS (m/z) [M + H]$^+$ calcd for C$_{14}$H$_{11}$Cl$_2$N$_2$ 277.0294, found 277.0366.

2-(2-Chloro-6-fluorophenyl)-6-methyl-1H-benzimidazole **(2e)**: white solid, mp 193–195 °C. ^{1}H NMR (500 MHz, DMSO-d$_6$, δ ppm): 12.74 (1H, s, –NH–), 8.19 (1H, d, J = 8.5 Hz, H$_{Ar}$), 8.18 (1H, d, J = 8.5 Hz, H$_{Ar}$), 7.50–7.33 (3H, m, H$_{Ar}$), 7.02 (1H, d, J = 7.5 Hz, H$_{Ar}$), 2.42 (3H, s, –CH$_3$). ^{13}C NMR (125 MHz, DMSO-d$_6$, δ ppm): 163.9, 162.0, 128.6, 128.5, 127.1, 126.9, 118.3, 116.0, 115.8, 111.1, 21.3. LC-MS (m/z) [M − H]$^-$ calcd for C$_{14}$H$_9$ClFN$_2$ 259.0444, found 259.0794; [M + H]$^+$ calcd for C$_{14}$H$_{11}$ClFN$_2$ 261.0589, found 261.0896.

2-(3,4-Dimethoxyphenyl)-6-methyl-1H-benzimidazole **(2f)**: white solid, mp 228–230 °C. ^{1}H NMR (500 MHz, DMSO-d$_6$, δ ppm): 12.61 (1H, s, –NH–), 7.76 (1H, d, J = 2.0 Hz, H$_{Ar}$), 7.73 (1H, dd, J = 8.0, 2.0 Hz, H$_{Ar}$), 7.45 (1H, d, J = 8.0 Hz, H$_{Ar}$), 7.35 (1H, s, H$_{Ar}$), 7.12 (1H, d, J = 8.5 Hz, H$_{Ar}$), 7.00 (1H, dd, J = 8.5, 1.5 Hz, H$_{Ar}$), 3.88 (3H, s, –OCH$_3$), 3.84 (3H, s, –OCH$_3$), 2.43 (3H, s, –CH$_3$). ^{13}C NMR (125 MHz, DMSO-d$_6$, δ ppm): 151.6, 150.6, 149.4, 123.7, 123.4, 119.6, 112.3, 110.1, 56.1, 56.0, 21.8. LC-MS (m/z) [M − H]$^-$ calcd for C$_{16}$H$_{15}$N$_2$O$_2$ 267.1139, found 267.1076; [M + H]$^+$ calcd for C$_{16}$H$_{17}$N$_2$O$_2$ 269.1285, found 269.1175.

2-(4-Ethoxyphenyl)-6-methyl-1H-benzimidazole **(2g)**: yellow solid, mp 258–260 °C. ^{1}H NMR (500 MHz, DMSO-d$_6$, δ ppm): 12.57 (1H, s, –NH–), 8.06 (2H, d, J = 8.0 Hz, H$_{Ar}$), 7.48 (1H, d, J = 8.0 Hz, H$_{Ar}$), 7.36 (1H, d, J = 8.5 Hz, H$_{Ar}$), 7.27 (1H, s, H$_{Ar}$), 7.07 (2H, d, J = 8.5 Hz, H$_{Ar}$), 4.11 (2H, q, J = 7.0 Hz, –CH$_2$–), 2.42 (3H, s, –CH$_3$), 1.36 (3H, t, J = 7.0 Hz, –CH$_3$). ^{13}C NMR (125 MHz, DMSO-d$_6$, δ ppm): 159.8, 151.3, 150.8, 142.0, 135.2, 133.0, 131.3, 130.3, 127.9, 127.8, 123.4, 122.9, 122.7, 118.3, 118.0, 114.7, 110.8, 110.5, 63.3, 21.3, 14.6. LC-MS (m/z) [M − H]$^-$ calcd for C$_{16}$H$_{15}$N$_2$O 251.1190, found 251.0255; [M + H]$^+$ calcd for C$_{16}$H$_{17}$N$_2$O 253.1335, found 253.0133.

δ*2-Ethoxy-4-(6-methyl-1H-benzimidazol-2-yl)phenol* **(2h)**: brown solid, mp 223–225 °C. ^{1}H NMR (500 MHz, DMSO-d$_6$, δ ppm): 12.49 (1H, s, –NH–), 9.40 (1H, s, –OH), 7.70 (1H, s, H$_{Ar}$), 7.58 (1H, d, J = 8.0 Hz, H$_{Ar}$), 7.47 (1H, d, J = 8.0 Hz, H$_{Ar}$), 7.35 (1H, d, J = 8.0 Hz, H$_{Ar}$), 7.26 (1H, s, H$_{Ar}$), 6.91 (1H, d, J = 8.5 Hz, H$_{Ar}$), 4.14 (2H, q, J = 7.0 Hz, –CH$_2$–), 2.42 (3H, s, –CH$_3$), 1.40 (3H, t, J = 7.0 Hz, –CH$_3$). ^{13}C NMR (125 MHz, DMSO-d$_6$, δ ppm): 151.3, 148.5, 146.9, 144.2, 142.0, 135.2, 131.2, 130.2, 123.3, 122.9, 121.6, 121.2, 119.6, 119.5, 118.1, 117.9, 115.8, 111.5, 110.7, 110.4, 64.0, 63.8, 21.4, 14.8, 14.6. LC-MS (m/z) [M − H]$^-$ calcd for C$_{16}$H$_{15}$N$_2$O$_2$ 267.1139, found 267.0427; [M + H]$^+$ calcd for C$_{16}$H$_{17}$N$_2$O$_2$ 269.1285, found 269.0582.

2-(4-Fluorophenyl)-6-methyl-1H-benzimidazole **(2i)**: brown solid, mp 217–219 °C. ^{1}H NMR (500 MHz, DMSO-d$_6$, δ ppm): 12.74 (1H, s, –NH–), 7.63 (2H, d, J = 8.5 Hz, H$_{Ar}$), 7.58 (1H, d, J = 8.0 Hz, H$_{Ar}$), 7.53 (2H, d, J = 8.0 Hz, H$_{Ar}$), 7.50 (1H, s, H$_{Ar}$), 7.44 (1H, t, J = 8.5 Hz, H$_{Ar}$), 7.34 (1H, s, H$_{Ar}$), 7.10 (1H, d, J = 8.0 Hz, H$_{Ar}$), 7.07 (1H, d, J = 8.0 Hz, H$_{Ar}$), 2.44 (3H, s, –CH$_3$). ^{13}C NMR (125 MHz, DMSO-d$_6$, δ ppm): 161.7, 159.7, 142.9, 141.4, 134.5, 134.3, 132.5, 132.2, 130.6, 125.81, 125.78, 124.3, 123.2, 120.0, 119.8, 118.9, 118.8, 114.9, 114.8, 111.2, 111.1, 21.3. LC-MS (m/z) [M − H]$^-$ calcd for C$_{14}$H$_{10}$FN$_2$ 225.0834, found 225.0014; [M + H]$^+$ calcd for C$_{14}$H$_{12}$FN$_2$ 227.0979, found 227.1081.

2-(6-Methyl-1H-benzimidazol-2-yl)phenol **(2j)**: white solid, mp 250–252 °C. ^{1}H NMR (500 MHz, DMSO-d$_6$, δ ppm): 13.21 (1H, s, –NH–), 9.71 (1H, s, –OH), 8.04 (1H, d, J = 7.0 Hz, H$_{Ar}$), 7.60–7.37

(2H, m, H$_{Ar}$), 7.35 (1H, s, H$_{Ar}$), 7.10–7.07 (1H, m, H$_{Ar}$), 7.04 (1H, d, J = 8.5 Hz, H$_{Ar}$), 7.00 (1H, d, J = 7.5 Hz, H$_{Ar}$), 2.45 (3H, s, –CH$_3$). ^{13}C NMR (125 MHz, DMSO-d$_6$, δ ppm): 158.0, 151.5, 151.3, 141.2, 139.0, 133.4, 131.5, 131.3, 129.8, 129.7, 126.0, 124.7, 124.1, 124.0, 119.0, 117.1, 112.7, 111.2, 21.4, 21.1. LC-MS (m/z) [M − H]$^-$ calcd for C$_{14}$H$_{11}$N$_2$O 223.0877, found 223.0852; [M + H]$^+$ calcd for C$_{14}$H$_{13}$N$_2$O 225.1022, found 225.0894.

4-Bromo-2-(6-methyl-1H-benzimidazol-2-yl)phenol **(2k)**: white solid, mp 277–278 °C. ^{1}H NMR (500 MHz, DMSO-d$_6$, δ ppm): 13.31 (1H, s, –NH–), 9.72 (1H, s, –OH), 8.26 (1H, d, J = 2.0 Hz, H$_{Ar}$), 7.60–7.57 (1H, s, H$_{Ar}$), 7.50 (1H, dd, J = 9.0, 2.5 Hz, H$_{Ar}$), 7.40 (1H, s, H$_{Ar}$), 7.15–7.06 (1H, m, H$_{Ar}$), 7.00 (1H, d, J = 8.5 Hz, H$_{Ar}$), 2.45 (3H, s, –CH$_3$). ^{13}C NMR (125 MHz, DMSO-d$_6$, δ ppm): 157.0, 133.8, 128.2, 124.2, 119.4, 117.7, 114.7, 111.3, 110.1, 21.3. LC-MS (m/z) [M + H]$^+$ calcd for C$_{14}$H$_{12}$BrN$_2$O 303.0128, found 302.9765.

3-(6-Methyl-1H-benzimidazol-2-yl)phenol **(2l)**: yellow solid, mp 294–296 °C. ^{1}H NMR (500 MHz, DMSO-d$_6$, δ ppm): 12.67 (1H, s, –NH–), 9.70 (1H, s, –OH), 7.57 (1H, d, J = 8.5 Hz, H$_{Ar}$), 7.52 (1H, d, J = 8.0 Hz, H$_{Ar}$), 7.43 (1H, s, H$_{Ar}$), 7.33 (1H, t, J = 8.0 Hz, H$_{Ar}$), 7.29 (1H, s, H$_{Ar}$), 7.02 (1H, d, J = 8.0 Hz, H$_{Ar}$), 6.88 (1H, dd, J = 8.0, 2.0 Hz, H$_{Ar}$), 2.43 (3H, s, –CH$_3$). ^{13}C NMR (125 MHz, DMSO-d$_6$, δ ppm): 157.7, 131.5, 129.9, 118.4, 117.1, 116.8, 113.2, 110.0, 21.3. LC-MS (m/z) [M − H]$^-$ calcd for C$_{14}$H$_{11}$N$_2$O 223.0877, found 223.0852; [M + H]$^+$ calcd for C$_{14}$H$_{13}$N$_2$O 225.1022, found 225.0894.

2-Methoxy-5-(6-methyl-1H-benzimidazol-2-yl)phenol **(2m)**: yellow solid, mp 248–249 °C. ^{1}H NMR (500 MHz, DMSO-d$_6$, δ ppm): 12.69 (1H, s, –NH–), 9.25 (1H, s, –OH), 7.60 (1H, s, H$_{Ar}$), 7.56 (1H, dd, J = 8.5, 1.5 Hz, H$_{Ar}$), 7.41 (1H, d, J = 8.0 Hz, H$_{Ar}$), 7.31 (1H, s, H$_{Ar}$), 7.06 (1H, d, J = 8.5 Hz, H$_{Ar}$), 6.98 (1H, d, J = 8.5 Hz, H$_{Ar}$), 3.84 (3H, s, –OCH$_3$), 2.41 (3H, s, –CH$_3$). ^{13}C NMR (125 MHz, DMSO-d$_6$, δ ppm): 151.2, 149.2, 146.6, 130.8, 123.1, 117.8, 113.7, 112.1, 55.7, 21.3. LC-MS (m/z) [M − H]$^-$ calcd for C$_{15}$H$_{13}$N$_2$O$_2$ 253.0983, found 253.1013; [M + H]$^+$ calcd for C$_{15}$H$_{15}$N$_2$O$_2$ 255.1128, found 255.1011.

2-(3-Methoxyphenyl)-6-methyl-1H-benzimidazole **(2n)**: white solid, mp 202–204 °C. ^{1}H NMR (500 MHz, DMSO-d$_6$, δ ppm): 12.79 (1H, s, –NH–), 7.74 (1H, d, J = 8.0 Hz, H$_{Ar}$), 7.73 (1H, d, J = 1.5 Hz, H$_{Ar}$), 7.48 (1H, d, J = 6.5 Hz, H$_{Ar}$), 7.44 (1H, t, J = 8.0 Hz, H$_{Ar}$), 7.38 (1H, s, H$_{Ar}$), 7.05–7.02 (2H, m, H$_{Ar}$), 3.85 (3H, s, –OCH$_3$), 2.42 (3H, s, –CH$_3$). ^{13}C NMR (125 MHz, DMSO-d$_6$, δ ppm): 159.8, 150.9, 131.6, 130.2, 123.8, 118.8, 115.8, 111.4, 55.4, 21.4. LC-MS (m/z) [M − H]$^-$ calcd for C$_{15}$H$_{13}$N$_2$O 237.1033, found 237.1105; [M + H]$^+$ calcd for C$_{15}$H$_{15}$N$_2$O 239.1179, found 239.0899.

6-Methyl-2-(4-(methylthio)phenyl)-1H-benzimidazole **(2o)**: brown solid, mp 94–95 °C. ^{1}H NMR (500 MHz, DMSO-d$_6$, δ ppm): 12.65 (1H, s, –NH–), 8.09 (2H, d, J = 8.5 Hz, H$_{Ar}$), 7.46 (1H, d, J = 8.0 Hz, H$_{Ar}$), 7.41 (2H, d, J = 8.5 Hz, H$_{Ar}$), 7.36 (1H, s, H$_{Ar}$), 7.02 (1H, d, J = 8.0 Hz, H$_{Ar}$), 2.55 (3H, s, –SCH$_3$), 2.43 (3H, s, –CH$_3$). ^{13}C NMR (125 MHz, DMSO-d$_6$, δ ppm): 151.1, 140.9, 131.7, 127.2, 127.1, 126.2, 124.0, 21.2, 14.8. LC-MS (m/z) [M − H]$^-$ calcd for C$_{15}$H$_{13}$N$_2$S 253.0805, found 253.0834; [M + H]$^+$ calcd for C$_{15}$H$_{15}$N$_2$S 255.0950, found 255.0866.

6-Methyl-2-(3-nitrophenyl)-1H-benzimidazole **(2p)**: yellow solid, mp 200–201 °C. ^{1}H NMR (500 MHz, DMSO-d$_6$, δ ppm):

13.12 (1H, s, –NH–), 8.99 (1H, s, H_{Ar}), 8.59 (1H, d, J = 8.0 Hz, H_{Ar}), 8.32 (1H, dd, J = 8.0, 1.0 Hz, H_{Ar}), 7.84 (1H, t, J = 8.0 Hz, H_{Ar}), 7.55–7.39 (2H, m, H_{Ar}), 7.08 (1H, d, J = 7.5 Hz, H_{Ar}), 2.50 (3H, s, –CH$_3$). ^{13}C NMR (125 MHz, DMSO-d$_6$, δ ppm): 148.4, 132.3, 131.9, 130.7, 124.0, 120.7, 21.3. LC-MS (m/z) [M – H]$^-$ calcd for $C_{14}H_{10}N_3O_2$ 252.0779, found 252.0872; [M + H]$^+$ calcd for $C_{14}H_{12}N_3O_2$ 254.0924, found 254.0882.

6-Methyl-2-(4-nitrophenyl)-1H-benzimidazole (*2q*): yellow solid, mp 240–242 °C. ^{1}H NMR (500 MHz, DMSO-d$_6$, δ ppm): 13.14 (1H, s, –NH–), 8.60–8.30 (4H, m, H_{Ar}), 7.60–7.36 (2H, m, H_{Ar}), 7.16–7.02 (1H, m, H_{Ar}), 2.44 (3H, s, –CH$_3$). ^{13}C NMR (125 MHz, DMSO-d$_6$, δ ppm): 147.7, 136.2, 127.2, 124.3, 124.0, 119.0, 111.4, 21.3. LC-MS (m/z) [M + H]$^+$ calcd for $C_{14}H_{12}N_3O_2$ 254.0924, found 254.0874.

N,N-Dimethyl-4-(6-methyl-1H-benzimidazol-2-yl)aniline (*2r*): yellow solid, mp 246–248 °C. ^{1}H NMR (500 MHz, DMSO-d$_6$, δ ppm): 12.36 (1H, s, –NH–), 7.97 (2H, d, J = 8.5 Hz, H_{Ar}), 7.35–7.28 (2H, m, H_{Ar}), 6.95 (1H, d, J = 8.0 Hz, H_{Ar}), 6.83 (2H, d, J = 9.0 Hz, H_{Ar}), 2.99 (6H, s, –N(CH$_3$)$_2$), 2.50 (3H, s, –CH$_3$). ^{13}C NMR (125 MHz, DMSO-d$_6$, δ ppm): 151.1, 127.4, 122.7, 117.6, 111.8, 39.84, 21.3. LC-MS (m/z) [M + H]$^+$ calcd for $C_{16}H_{18}N_3$ 252.1495, found 252.1590.

2-(Anthracen-9-yl)-6-methyl-1H-benzimidazole (*2s*): yellow solid, mp 323–324 °C. ^{1}H NMR (500 MHz, DMSO-d$_6$, δ ppm): 13.02 (1H, s, –NH–), 8.84 (1H, s, H_{Ar}), 8.25 (2H, d, J = 8.5 Hz, H_{Ar}), 7.62 (4H, d, J = 8.5 Hz, H_{Ar}), 7.61–7.48 (3H, m, H_{Ar}), 7.33 (2H, q, J = 3.0 Hz, H_{Ar}), 2.43 (3H, s, –CH$_3$). ^{13}C NMR (125 MHz, DMSO-d$_6$, δ ppm): 150.2, 132.4, 130.6, 128.7, 128.2, 126.5, 125.8, 125.7, 125.3, 122.1, 118.5, 111.2, 21.9. LC-MS (m/z) [M – H]$^-$ calcd for $C_{22}H_{15}N_2$ 307.1241, found 307.1253; [M + H]$^+$ calcd for $C_{22}H_{17}N_2$ 309.1386, found 308.1327.

2-(Benzo[d][1,3]dioxol-5-yl)-6-methyl-1H-benzimidazole (*2t*): yellow solid, mp 258–259 °C. ^{1}H NMR (500 MHz, DMSO-d$_6$, δ ppm): 12.81 (1H, s, –NH–), 7.76 (1H, dd, J = 8.0, 2.0 Hz, H_{Ar}), 7.67 (1H, d, J = 1.5 Hz, H_{Ar}), 7.60 (1H, d, J = 7.5 Hz, H_{Ar}), 7.51 (1H, d, J = 7.0 Hz, H_{Ar}), 7.17 (1H, t, J = 7.5 Hz, H_{Ar}), 7.05 (1H, d, J = 8.0 Hz, H_{Ar}), 6.14 (2H, s, –CH$_2$–), 2.41 (3H, s, –CH$_3$). ^{13}C NMR (125 MHz, DMSO-d$_6$, δ ppm): 151.2, 148.6, 147.8, 143.9, 134.6, 124.5, 122.0, 121.6, 120.3, 118.5, 111.5, 108.6, 106.4, 101.5, 21.8. LC-MS (m/z) [M – H]$^-$ calcd for $C_{15}H_{11}N_2O_2$ 251.0826, found 251.0843; [M + H]$^+$ calcd for $C_{15}H_{13}N_2O_2$ 253.0972, found 253.0986.

2-(Furan-2-yl)-6-methyl-1H-benzimidazole (*2u*): brown solid, mp 191–193 °C. ^{1}H NMR (500 MHz, DMSO-d$_6$, δ ppm): 12.77 (1H, s, –NH–), 7.92 (1H, d, J = 4.0 Hz, H_{Ar}), 7.49–7.29 (2H, m, H_{Ar}), 7.16 (1H, d, J = 4.0 Hz, H_{Ar}), 7.02 (1H, d, J = 8.0 Hz, H_{Ar}), 6.72 (1H, dd, J = 4.0, 2.0 Hz, H_{Ar}), 2.42 (3H, s, –CH$_3$). ^{13}C NMR (125 MHz, DMSO-d$_6$, δ ppm): 146.2, 144.9, 143.7, 142.2, 132.5, 123.9, 118.8, 112.7, 111.5, 110.6, 21.8. LC-MS (m/z) [M – H]$^-$ calcd for $C_{12}H_9N_2O$ 197.0720, found 197.0773; [M + H]$^+$ calcd for $C_{12}H_{11}N_2O$ 199.0866, found 199.0822.

6-Methyl-2-(pyridin-3-yl)-1H-benzimidazole (*2v*): yellow solid, mp 246–248 °C. ^{1}H NMR (500 MHz, DMSO-d$_6$, δ ppm): 12.92 (1H, s, –NH–), 9.32 (1H, d, J = 1.5 Hz, H_{Ar}), 8.66 (1H, d, J = 3.5 Hz, H_{Ar}), 8.47 (1H, d, J = 8.0 Hz, H_{Ar}), 7.58–7.56 (1H, m, H_{Ar}), 7.48–7.41 (1H, m, H_{Ar}), 7.35 (1H, s, H_{Ar}), 7.06–7.04 (1H, m, H_{Ar}), 2.44 (3H, s, –CH$_3$). ^{13}C NMR (125 MHz, DMSO-d$_6$, δ ppm): 150.3,

148.4, 147.4, 133.6, 126.3, 124.0, 123.6, 118.6, 111.1, 99.4, 89.2, 21.3. LC-MS (m/z) [M + H]$^+$ calcd for $C_{13}H_{12}N_3$ 210.1026, found 210.0951.

6-Methyl-2-(pyridin-4-yl)-1H-benzimidazole (*2w*): brown solid, mp 149–150 °C. ^{1}H NMR (500 MHz, DMSO-d$_6$, δ ppm): 13.09 (1H, s, –NH–), 8.74 (2H, d, J = 5.5 Hz, H_{Ar}), 8.06 (2H, d, J = 5.5 Hz, H_{Ar}), 7.60–7.40 (2H, m, H_{Ar}), 7.09 (1H, d, J = 6.0 Hz, H_{Ar}), 2.44 (3H, s, –CH$_3$). ^{13}C NMR (125 MHz, DMSO-d$_6$, δ ppm): 150.4, 137.2, 133.1, 120.2, 119.1, 111.3, 21.3. LC-MS (m/z) [M – H]$^-$ calcd for $C_{13}H_{10}N_3$ 208.0880, found 208.1029; [M + H]$^+$ calcd for $C_{13}H_{12}N_3$ 210.1026, found 210.0911.

4.2.2 General procedure for the preparation of N,2,6-trisubstituted 1H-benzimidazole derivatives (3a–l and 4a–k)

4.2.2.1 Refluxing method. The mixture of 2,6-disubstituted 1H-benzimidazole derivatives **1–2** (1 mmol), potassium carbonate (1 mmol), and substituted halides (1.2 mmol) in acetonitrile (10 mL) was heated at 80 °C for 12–24 h and monitored by TLC. After cooling down, the mixture was poured into cooled water and filtered off in a Büchner funnel. The resulting solid was purified by silica gel column chromatography using hexane/ethyl acetate as eluent. Yields: 35–86%.

4.2.2.2 Microwave-assisted method. The mixture of 2,6-disubstituted 1H-benzimidazole derivatives **1–2** (1 mmol), potassium carbonate (1 mmol), and substituted halides (1.2 mmol) in acetonitrile (10 mL) was irradiated at a power of 300 W for 20–60 min at 80 °C. After cooling down, the mixture was poured into cooled water and filtered off in a Büchner funnel. The resulting solid was purified by silica gel column chromatography using hexane/ethyl acetate as eluent. Yields: 46–98%.

1-Allyl-2-(4-chlorophenyl)-1H-benzimidazole (*3a*): yellow solid, mp 99–101 °C. IR (ν, cm^{-1}): 1601 (C=N), 1454 (C=C), 842 (C–Cl). ^{1}H NMR (500 MHz, DMSO-d$_6$, δ ppm): 7.80 (2H, d, J = 8.5 Hz, H_{Ar}), 7.71 (1H, d, J = 7.0 Hz, H_{Ar}), 7.63 (2H, d, J = 8.5 Hz, H_{Ar}), 7.54 (1H, d, J = 7.5 Hz, H_{Ar}), 7.31–7.25 (2H, m, H_{Ar}), 6.10–6.03 (1H, m, –CH=), 5.20 (1H, d, J = 10.5 Hz, =CH$_2$), 4.93 (2H, s, –CH$_2$–), 4.88 (1H, d, J = 17.5 Hz, =CH$_2$). ^{13}C NMR (125 MHz, DMSO-d$_6$, δ ppm): 151.8, 142.5, 135.8, 134.7, 133.3, 130.7, 128.9, 128.8, 122.7, 122.2, 119.2, 116.6, 111.0, 46.6. LC-MS (m/z) [M – H]$^-$ calcd for $C_{16}H_{12}ClN_2$ 267.0694, found 267.0917; [M + H]$^+$ calcd for $C_{16}H_{14}ClN_2$ 269.0840, found 269.0883.

1-Allyl-2-(3,4-dichlorophenyl)-1H-benzimidazole (*3b*): yellow solid, mp 97–99 °C. IR (ν, cm^{-1}): 1607 (C=N), 1450 (C=C), 731 (C–Cl). ^{1}H NMR (500 MHz, DMSO-d$_6$, δ ppm): 8.02 (1H, d, J = 1.0 Hz, H_{Ar}), 7.84 (1H, d, J = 8.0 Hz, H_{Ar}), 7.76 (1H, dd, J = 8.0, 1.0 Hz, H_{Ar}), 7.72 (1H, d, J = 7.5 Hz, H_{Ar}), 7.56 (1H, d, J = 7.5 Hz, H_{Ar}), 7.33–7.26 (2H, m, H_{Ar}), 6.11–6.04 (1H, m, –CH=), 5.21 (1H, d, J = 10.5 Hz, =CH$_2$), 4.96 (2H, s, –CH$_2$–), 4.89 (1H, d, J = 17.0 Hz, =CH$_2$). ^{13}C NMR (125 MHz, DMSO-d$_6$, δ ppm): 150.5, 142.4, 135.9, 133.3, 132.7, 131.5, 131.0, 130.62, 130.59, 128.9, 123.0, 122.4, 119.4, 116.7, 111.1, 46.6. LC-MS (m/z) [M + H]$^+$ calcd for $C_{16}H_{13}Cl_2N_2$ 303.0450, found 303.1268.

1-Allyl-2-(3,4-dimethoxyphenyl)-1H-benzimidazole (*3c*): yellow solid, mp 198–200 °C. IR (ν, cm^{-1}): 1586 (C=N), 1468 (C=C), 1253 (C–O). ^{1}H NMR (500 MHz, DMSO-d$_6$, δ ppm): 7.68 (1H, dd, J = 8.5, 2.0 Hz, H_{Ar}), 7.50 (1H, dd, J = 8.5, 1.5 Hz, H_{Ar}), 7.34 (1H, s, H_{Ar}), 7.31 (1H, dd, J = 8.0, 2.0 Hz, H_{Ar}), 7.27–7.22 (2H, m, H_{Ar}), 7.14 (1H, d, J = 8.5 Hz, H_{Ar}), 6.16–6.09 (1H, m, –CH=), 5.24

(1H, d, $J = 10.0$ Hz, $=CH_2$), 4.94 (2H, s, $-CH_2-$), 4.93 (1H, d, $J = 15.5$ Hz, $=CH_2$), 3.85 (3H, s, $-OCH_3$), 3.82 (3H, s, $-OCH_3$). ^{13}C NMR (125 MHz, DMSO-d_6, δ ppm): 153.0, 150.1, 148.6, 142.5, 135.9, 133.6, 122.3, 122.2, 121.9, 121.4, 118.9, 116.4, 112.4, 111.6, 110.7, 55.6, 55.5, 46.6. LC-MS (m/z) $[M - H]^-$ calcd for $C_{18}H_{17}N_2O_2$ 293.1296, found 293.1032; $[M + H]^+$ calcd for $C_{18}H_{19}N_2O_2$ 295.1441, found 295.1241.

1-Allyl-2-(4-nitrophenyl)-1H-benzimidazole (3d): yellow solid, mp 127–129 °C. IR (ν, cm^{-1}): 1599 (C=N), 1516 (C=C), 1344 (N=O). ^1H NMR (500 MHz, DMSO-d_6, δ ppm): 8.41 (2H, d, $J = 8.5$ Hz, H_{Ar}), 8.08 (2H, d, $J = 8.5$ Hz, H_{Ar}), 7.76 (1H, d, $J = 7.5$ Hz, H_{Ar}), 7.60 (1H, d, $J = 8.0$ Hz, H_{Ar}), 7.36–7.29 (2H, m, H_{Ar}), 6.11–6.06 (1H, m, $-CH=$), 5.22 (1H, d, $J = 10.0$ Hz, $=CH_2$), 5.01 (1H, s, $-CH_2-$), 5.00 (1H, s, $-CH_2-$), 4.90 (1H, d, $J = 17.0$ Hz, $=CH_2$). ^{13}C NMR (125 MHz, DMSO-d_6, δ ppm): 150.7, 148.0, 142.5, 136.2, 136.1, 133.2, 130.2, 123.9, 123.3, 122.6, 119.6, 116.8, 111.2, 46.7. LC-MS (m/z) $[M + H]^+$ calcd for $C_{16}H_{14}N_3O_2$ 280.1081, found 280.2779.

1-Benzyl-2-(4-chlorophenyl)-1H-benzimidazole (3e): yellow solid, mp 148–149 °C. IR (ν, cm^{-1}): 1514 (C=N), 1425 (C=C), 754 (C–Cl). ^1H NMR (500 MHz, DMSO-d_6, δ ppm): 7.76–7.73 (3H, m, H_{Ar}), 7.59 (2H, d, $J = 8.5$ Hz, H_{Ar}), 7.48 (1H, d, $J = 8.5$ Hz, H_{Ar}), 7.29–7.23 (5H, m, H_{Ar}), 6.99 (2H, d, $J = 7.5$ Hz, H_{Ar}), 5.59 (2H, s, $-CH_2-$). ^{13}C NMR (125 MHz, DMSO-d_6, δ ppm): 152.1, 142.6, 136.8, 136.0, 134.7, 130.8, 130.0, 128.9, 128.8, 127.5, 126.1, 122.9, 122.3, 119.3, 111.1, 47.4. LC-MS (m/z) $[M + H]^+$ calcd for $C_{20}H_{16}ClN_2$ 319.0997, found 319.0913.

1-Benzyl-2-(3,4-dichlorophenyl)-1H-benzimidazole (3f): yellow solid, mp 113–114 °C. IR (ν, cm^{-1}): 1545 (C=N), 1409 (C=C), 743 (C–Cl). ^1H NMR (500 MHz, DMSO-d_6, δ ppm): 7.94 (1H, d, $J = 1.5$ Hz, H_{Ar}), 7.78 (1H, d, $J = 8.0$ Hz, H_{Ar}), 7.75 (1H, dd, $J = 9.0$, 1.5 Hz, H_{Ar}), 7.70 (1H, dd, $J = 8.5$, 2.0 Hz, H_{Ar}), 7.53 (1H, dd, $J = 9.0$, 2.0 Hz, H_{Ar}), 7.30–7.25 (4H, m, H_{Ar}), 7.23 (1H, d, $J = 7.0$ Hz, H_{Ar}), 7.00 (2H, d, $J = 7.0$ Hz, H_{Ar}), 5.62 (2H, s, $-CH_2-$). ^{13}C NMR (125 MHz, DMSO-d_6, δ ppm): 150.7, 142.5, 136.7, 136.1, 132.7, 131.6, 131.0, 130.8, 130.7, 129.0, 128.8, 127.6, 126.1, 123.2, 122.5, 119.5, 111.2, 47.5. LC-MS (m/z) $[M + H]^+$ calcd for $C_{20}H_{15}Cl_2N_2$ 353.0607, found 353.0698.

1-Benzyl-2-(3,4-dimethoxyphenyl)-1H-benzimidazole (3g): yellow solid, mp 140–141 °C. IR (ν, cm^{-1}): 1601 (C=N), 1461 (C=C). ^1H NMR (500 MHz, DMSO-d_6, δ ppm): 7.71 (1H, d, $J = 7.0$ Hz, H_{Ar}), 7.44 (1H, d, $J = 7.5$ Hz, H_{Ar}), 7.32 (2H, t, $J = 7.5$ Hz, H_{Ar}), 7.27–7.20 (5H, m, H_{Ar}), 7.08 (1H, d, $J = 8.5$ Hz, H_{Ar}), 7.04 (2H, d, $J = 7.5$ Hz, H_{Ar}), 5.59 (2H, s, $-CH_2-$), 3.81 (3H, s, $-OCH_3$), 3.66 (3H, s, $-OCH_3$). ^{13}C NMR (125 MHz, DMSO-d_6, δ ppm): 153.3, 150.1, 148.6, 142.6, 137.2, 136.1, 128.8, 127.4, 125.9, 122.5, 122.3, 122.1, 121.6, 119.0, 112.3, 111.7, 110.8, 55.6, 55.3, 47.5. LC-MS (m/z) $[M + H]^+$ calcd for $C_{22}H_{21}N_2O_2$ 345.1598, found 345.1474.

1-Benzyl-2-(4-ethoxyphenyl)-1H-benzimidazole (3h): yellow solid, mp 227–229 °C. IR (ν, cm^{-1}): 1608 (C=N), 1457 (C=C), 1257 (C–O). ^1H NMR (500 MHz, DMSO-d_6, δ ppm): 7.69 (1H, d, $J = 7.5$ Hz, H_{Ar}), 7.65 (2H, d, $J = 8.0$ Hz, H_{Ar}), 7.42 (1H, d, $J = 7.5$ Hz, H_{Ar}), 7.29 (2H, d, $J = 7.0$ Hz, H_{Ar}), 7.25–7.19 (3H, m, H_{Ar}), 7.05 (2H, d, $J = 8.0$ Hz, H_{Ar}), 7.01 (2H, d, $J = 7.0$ Hz, H_{Ar}), 5.37 (2H, s, $-CH_2-$), 4.09 (2H, q, $J = 6.5$ Hz, $-CH=$), 1.34 (3H, t, $J = 6.5$ Hz, $-CH=$). ^{13}C NMR (125 MHz, DMSO-d_6, δ ppm): 159.6,

153.2, 142.7, 137.0, 135.9, 130.4, 128.7, 127.4, 126.0, 122.3, 122.1, 122.0, 119.0, 114.6, 110.8, 63.2, 47.4, 14.5. LC-MS (m/z) $[M - H]^-$ calcd for $C_{22}H_{19}N_2O$ 327.1503, found 327.1003; $[M + H]^+$ calcd for $C_{22}H_{21}N_2O$ 329.1648, found 329.1559.

1-Benzyl-2-(4-fluorophenyl)-1H-benzimidazole (3i): yellow solid, mp 129–130 °C. IR (ν, cm^{-1}): 1572 (C=N), 1397 (C=C), 1220 (C–F). ^1H NMR (500 MHz, DMSO-d_6, δ ppm): 7.77 (1H, d, $J = 8.5$ Hz, H_{Ar}), 7.67 (1H, d, $J = 8.5$ Hz, H_{Ar}), 7.72 (1H, dd, $J = 8.0$, 1.0 Hz, H_{Ar}), 7.48 (1H, dd, $J = 8.0$, 1.5 Hz, H_{Ar}), 7.34 (2H, t, $J = 8.5$ Hz, H_{Ar}), 7.30–7.23 (5H, m, H_{Ar}), 6.99 (2H, d, $J = 7.5$ Hz, H_{Ar}), 5.58 (2H, s, $-CH_2-$). ^{13}C NMR (125 MHz, DMSO-d_6, δ ppm): 163.9, 161.9, 152.3, 142.5, 136.8, 135.9, 131.42, 131.36, 128.8, 127.5, 126.64, 126.61, 126.1, 122.8, 122.3, 119.2, 116.0, 115.8, 111.1, 47.4. LC-MS (m/z) $[M + H]^+$ calcd for $C_{20}H_{16}FN_2$ 303.1292, found 303.1268.

1-Benzyl-2-(3-methoxyphenyl)-1H-benzimidazole (3j): yellow solid, mp 107–108 °C. IR (ν, cm^{-1}): 1568 (C=N), 1453 (C=C). ^1H NMR (500 MHz, DMSO-d_6, δ ppm): 7.74 (1H, dd, $J = 7.0$, 1.0 Hz, H_{Ar}), 7.47–7.42 (2H, m, H_{Ar}), 7.31–7.28 (3H, m, H_{Ar}), 7.26–7.23 (4H, m, H_{Ar}), 7.09 (1H, dd, $J = 8.0$, 2.0 Hz, H_{Ar}), 7.02 (2H, d, $J = 7.5$ Hz, H_{Ar}), 5.59 (2H, s, $-CH_2-$), 3.72 (3H, s, $-OCH_3$). ^{13}C NMR (125 MHz, DMSO-d_6, δ ppm): 159.2, 153.0, 142.6, 137.0, 135.9, 131.3, 129.9, 128.8, 127.4, 126.0, 122.7, 122.2, 121.2, 119.3, 115.8, 114.2, 111.0, 55.1, 47.5. LC-MS (m/z) $[M + H]^+$ calcd for $C_{21}H_{19}N_2O$ 315.1492, found 315.1444.

1-Benzyl-2-(4-nitrophenyl)-1H-benzimidazole (3k): yellow solid, mp 191–192 °C. IR (ν, cm^{-1}): 1602 (C=N), 1498 (C=C), 1343 (N=O). ^1H NMR (500 MHz, DMSO-d_6, δ ppm): 8.35 (2H, d, $J = 9.0$ Hz, H_{Ar}), 8.04 (2H, d, $J = 8.5$ Hz, H_{Ar}), 7.78 (1H, d, $J = 9.0$ Hz, H_{Ar}), 7.56 (1H, d, $J = 9.0$ Hz, H_{Ar}), 7.31–7.21 (5H, m, H_{Ar}), 6.99 (2H, d, $J = 7.5$ Hz, H_{Ar}), 5.67 (2H, s, $-CH_2-$). ^{13}C NMR (125 MHz, DMSO-d_6, δ ppm): 151.0, 148.0, 142.6, 136.6, 136.3, 136.2, 130.3, 128.8, 127.6, 126.1, 123.9, 123.5, 122.7, 119.7, 111.4, 47.6. LC-MS (m/z) $[M + H]^+$ calcd for $C_{20}H_{16}N_3O_2$ 330.1237, found 330.1215.

1-(4-Chlorobenzyl)-2-(4-chlorophenyl)-1H-benzimidazole (3l): white solid, mp 147–148 °C. IR (ν, cm^{-1}): 1557 (C=N), 1445 (C=C), 744 (C–Cl). ^1H NMR (500 MHz, DMSO-d_6, δ ppm): 7.76 (1H, d, $J = 8.0$ Hz, H_{Ar}), 7.68 (2H, d, $J = 8.5$ Hz, H_{Ar}), 7.58 (2H, d, $J = 8.5$ Hz, H_{Ar}), 7.50 (1H, d, $J = 7.5$ Hz, H_{Ar}), 7.42 (1H, d, $J = 7.5$ Hz, H_{Ar}), 7.33–7.20 (4H, m, H_{Ar}), 6.62 (1H, d, $J = 8.0$ Hz, H_{Ar}), 5.61 (2H, s, $-CH_2-$). ^{13}C NMR (125 MHz, DMSO-d_6, δ ppm): 142.5, 135.9, 134.8, 133.8, 131.3, 130.6, 129.7, 129.4, 128.9, 128.8, 127.7, 127.3, 123.0, 122.5, 119.4, 110.9, 45.8. LC-MS (m/z) $[M + H]^+$ calcd for $C_{20}H_{15}Cl_2N_2$ 353.0607, found 353.0698.

1-Allyl-2-(4-chlorophenyl)-6-methyl-1H-benzimidazole (4a): white solid, mp 138–140 °C. IR (ν, cm^{-1}): 1608 (C=N), 1460 (C=C), 803 (C–Cl). ^1H NMR (500 MHz, DMSO-d_6, δ ppm): 7.78 (2H, d, $J = 8.0$ Hz, H_{Ar}), 7.63 (2H, d, $J = 8.0$ Hz, H_{Ar}), 7.58 (1H, d, $J = 8.0$ Hz, H_{Ar}), 7.32 (1H, s, H_{Ar}), 7.09 (1H, d, $J = 8.5$ Hz, H_{Ar}), 6.09–6.04 (1H, m, $-CH=$), 5.20 (1H, d, $J = 10.0$ Hz, $=CH_2$), 4.89 (2H, s, $-CH_2-$), 4.84 (1H, d, $J = 20.5$ Hz, $=CH_2$), 2.45 (3H, s, $-CH_3$). ^{13}C NMR (125 MHz, DMSO-d_6, δ ppm): 151.3, 140.6, 136.1, 134.5, 133.4, 132.2, 130.6, 129.0, 124.2, 123.8, 118.9, 116.5, 110.6, 46.6, 21.4. LC-MS (m/z) $[M - H]^-$ calcd for $C_{17}H_{14}ClN_2$ 281.0851, found 281.0440; $[M + H]^+$ calcd for $C_{17}H_{16}ClN_2$ 283.0997, found 283.0922.

1-Allyl-6-methyl-2-(4-nitrophenyl)-1H-benzimidazole **(4b)**: orange solid, mp 100–102 °C. IR (ν, cm^{-1}): 1601 (C=N), 1515 (C=C), 1340 (N=O). ^{1}H NMR (500 MHz, DMSO-d$_6$, δ ppm): 8.38 (2H, d, J = 8.5 Hz, H$_{Ar}$), 8.05 (2H, d, J = 8.0 Hz, H$_{Ar}$), 7.46 (1H, d, J = 8.5 Hz, H$_{Ar}$), 7.38 (1H, s, H$_{Ar}$), 7.15 (1H, d, J = 9.0 Hz, H$_{Ar}$), 6.11–6.04 (1H, m, –CH=), 5.21 (1H, d, J = 9.5 Hz, =CH$_2$), 4.96 (2H, s, –CH$_2$–), 4.87 (1H, d, J = 17.5 Hz, =CH$_2$), 2.46 (3H, s, –CH$_3$). ^{13}C NMR (125 MHz, DMSO-d$_6$, δ ppm): 150.2, 147.8, 142.9, 136.4, 134.3, 133.2, 131.7, 130.1, 124.9, 123.8, 119.2, 116.7, 110.8, 46.7, 21.5. LC-MS (m/z) [M – H]$^-$ calcd for C$_{17}$H$_{14}$N$_3$O$_2$ 292.1092, found 292.0119; [M + H]$^+$ calcd for C$_{17}$H$_{16}$N$_3$O$_2$ 294.1237, found 294.0211.

1-Benzyl-2-(4-chlorophenyl)-6-methyl-1H-benzimidazole **(4c)**: yellow solid, mp 123–125 °C. IR (ν, cm^{-1}): 1563 (C=N), 1500 (C=C), 750 (C–Cl). ^{1}H NMR (500 MHz, DMSO-d$_6$, δ ppm): 7.74–7.71 (2H, m, H$_{Ar}$), 7.62–7.56 (3H, m, H$_{Ar}$), 7.31–7.24 (4H, m, H$_{Ar}$), 7.10 (1H, d, J = 8.5 Hz, H$_{Ar}$), 6.98 (2H, d, J = 7.0 Hz, H$_{Ar}$), 5.55 (2H, s, –CH$_2$–), 2.42 (3H, s, –CH$_3$). ^{13}C NMR (125 MHz, DMSO-d$_6$, δ ppm): 151.6, 140.8, 136.9, 136.3, 134.5, 132.4, 130.7, 129.1, 128.9, 128.8, 127.5, 126.0, 123.9, 119.0, 110.7, 47.3, 21.4. LC-MS (m/z) [M + H]$^+$ calcd for C$_{21}$H$_{18}$ClN$_2$ 333.1153, found 333.1102.

1-Benzyl-2-(3,4-dichlorophenyl)-6-methyl-1H-benzimidazole **(4d)**: brown solid, mp 138–140 °C. IR (ν, cm^{-1}): 1613 (C=N), 1459 (C=C), 714 (C–Cl). ^{1}H NMR (500 MHz, DMSO-d$_6$, δ ppm): 7.93 (1H, dd, J = 8.0, 2.0 Hz, H$_{Ar}$), 7.71 (1H, d, J = 2.0 Hz, H$_{Ar}$), 7.63 (1H, d, J = 8.5 Hz, H$_{Ar}$), 7.54 (1H, s, H$_{Ar}$), 7.41 (1H, d, J = 8.5 Hz, H$_{Ar}$), 7.35–7.23 (3H, m, H$_{Ar}$), 7.11 (1H, d, J = 9.0 Hz, H$_{Ar}$), 7.00 (2H, d, J = 8.5 Hz, H$_{Ar}$), 5.60 (2H, s, –CH$_2$–), 2.43 (3H, s, –CH$_3$). ^{13}C NMR (125 MHz, DMSO-d$_6$, δ ppm): 151.1, 143.3, 141.1, 137.4, 136.9, 134.8, 133.2, 132.2, 131.5, 131.2, 129.4, 128.0, 126.5, 125.2, 124.6, 119.6, 111.3, 48.0, 22.0. LC-MS (m/z) [M + H]$^+$ calcd for C$_{21}$H$_{17}$Cl$_2$N$_2$ 367.0763, found 367.0701.

1-Benzyl-2-(4-fluorophenyl)-6-methyl-1H-benzimidazole **(4e)**: brown solid, mp 111–112 °C. IR (ν, cm^{-1}): 1607 (C=N), 1479 (C=C), 1219 (C–F). ^{1}H NMR (500 MHz, DMSO-d$_6$, δ ppm): 7.75 (2H, d, J = 8.5 Hz, H$_{Ar}$), 7.61 (1H, d, J = 8.0 Hz, H$_{Ar}$), 7.52 (1H, s, H$_{Ar}$), 7.39–7.23 (5H, m, H$_{Ar}$), 7.08 (1H, d, J = 9.0 Hz, H$_{Ar}$), 6.99 (2H, d, J = 8.5 Hz, H$_{Ar}$), 5.55 (2H, s, –CH$_2$–), 2.43 (3H, s, –CH$_3$). ^{13}C NMR (125 MHz, DMSO-d$_6$, δ ppm): 164.5, 152.7, 143.3, 141.2, 137.4, 134.5, 132.7, 131.8, 129.3, 127.9, 126.5, 124.7, 119.3, 116.4, 111.2, 47.9, 21.9. LC-MS (m/z) [M + H]$^+$ calcd for C$_{21}$H$_{18}$FN$_2$ 317.1449, found 317.1362.

1-Benzyl-6-methyl-2-(4-(methylthio)phenyl)-1H-benzimidazole **(4f)**: brown solid, mp 123–124 °C. IR (ν, cm^{-1}): 1599 (C=N), 1496 (C=C), 588 (C–S). ^{1}H NMR (500 MHz, DMSO-d$_6$, δ ppm): 7.65 (2H, d, J = 8.5 Hz, H$_{Ar}$), 7.59 (1H, d, J = 8.0 Hz, H$_{Ar}$), 7.39–7.35 (3H, m, H$_{Ar}$), 7.33–7.23 (3H, m, H$_{Ar}$), 7.08 (1H, d, J = 9.0 Hz, H$_{Ar}$), 7.00 (2H, d, J = 8.5 Hz, H$_{Ar}$), 5.56 (2H, s, –CH$_2$–), 2.52 (3H, s, –SCH$_3$), 2.42 (3H, s, –CH$_3$). ^{13}C NMR (125 MHz, DMSO-d$_6$, δ ppm): 153.8, 150.8, 141.4, 136.6, 136.5, 129.6, 128.4, 127.2, 126.1, 125.7, 121.7, 119.5, 116.3, 111.4, 110.1, 47.5, 21.8, 14.9. LC-MS (m/z) [M + H]$^+$ calcd for C$_{22}$H$_{21}$N$_2$S 345.1420, found 345.1344.

1-Benzyl-6-methyl-2-(4-nitrophenyl)-1H-benzimidazole **(4g)**: yellow solid, mp 165–167 °C. IR (ν, cm^{-1}): 1560 (C=N), 1513 (C=C), 1341 (N=O). ^{1}H NMR (500 MHz, DMSO-d$_6$, δ ppm): 8.34 (2H, d, J = 8.5 Hz, H$_{Ar}$), 8.02 (2H, d, J = 8.5 Hz, H$_{Ar}$), 7.66 (1H, d, J = 8.0 Hz, H$_{Ar}$), 7.36 (1H, s, H$_{Ar}$), 7.30–7.21 (3H, m, H$_{Ar}$), 7.12 (1H, d, J = 7.5 Hz, H$_{Ar}$), 6.98 (2H, d, J = 7.0 Hz, H$_{Ar}$), 5.64 (2H, s, –CH$_2$–), 2.44 (3H, s, –CH$_3$). ^{13}C NMR (125 MHz, DMSO-d$_6$, δ ppm): 150.9, 147.9, 143.0, 140.8, 136.7, 134.4, 133.1, 131.9, 130.3, 128.9, 127.6, 126.1, 124.4, 119.3, 111.0, 47.6, 21.5. LC-MS (m/z) [M + H]$^+$ calcd for C$_{21}$H$_{18}$N$_3$O$_2$ 344.1394, found 344.1229.

1-(2-Chlorobenzyl)-2-(4-chlorophenyl)-6-methyl-1H-benzimidazole **(4h)**: yellow solid, mp 137–138 °C. IR (ν, cm^{-1}): 1634 (C=N), 1468 (C=C), 754 (C–Cl). ^{1}H NMR (500 MHz, DMSO-d$_6$, δ ppm): 7.65 (2H, d, J = 8.5 Hz, H$_{Ar}$), 7.56 (2H, d, J = 8.5 Hz, H$_{Ar}$), 7.51 (1H, d, J = 9.0 Hz, H$_{Ar}$), 7.33–7.20 (3H, m, H$_{Ar}$), 7.20 (1H, d, J = 8.5 Hz, H$_{Ar}$), 7.10 (1H, d, J = 8.0 Hz, H$_{Ar}$), 6.58 (1H, t, J = 8.5 Hz, H$_{Ar}$), 5.56 (2H, s, –CH$_2$–), 2.43 (3H, s, –CH$_3$). ^{13}C NMR (125 MHz, DMSO-d$_6$, δ ppm): 152.1, 142.9, 136.2, 134.6, 134.0, 132.6, 131.6, 131.3, 130.5, 129.6, 128.8, 127.7, 127.2, 124.5, 124.1, 119.1, 110.5, 45.8, 21.4. LC-MS (m/z) [M – H]$^-$ calcd for C$_{13}$H$_{10}$N$_3$ 365.0618, found 364.9981; [M + H]$^+$ calcd for C$_{21}$H$_{17}$Cl$_2$N$_2$ 367.0763, found 367.0769.

1-(2-Chlorobenzyl)-6-methyl-2-(4-nitrophenyl)-1H-benzimidazole **(4i)**: yellow solid, mp 215–217 °C. IR (ν, cm^{-1}): 1600 (C=N), 1518 (C=C), 1345 (N=O). ^{1}H NMR (500 MHz, DMSO-d$_6$, δ ppm): 8.33 (2H, d, J = 8.5 Hz, H$_{Ar}$), 7.96 (2H, d, J = 9.0 Hz, H$_{Ar}$), 7.69 (1H, d, J = 8.5 Hz, H$_{Ar}$), 7.52 (1H, s, H$_{Ar}$), 7.35–7.29 (2H, m, H$_{Ar}$), 7.21 (1H, d, J = 8.5 Hz, H$_{Ar}$), 7.15 (1H, d, J = 8.0 Hz, H$_{Ar}$), 6.64 (1H, d, J = 8.0 Hz, H$_{Ar}$), 5.65 (2H, s, –CH$_2$–), 2.44 (3H, s, –CH$_3$). ^{13}C NMR (125 MHz, DMSO-d$_6$, δ ppm): 151.1, 147.9, 140.8, 136.4, 134.3, 133.7, 132.0, 131.4, 130.1, 129.7, 127.8, 127.5, 125.1, 124.5, 123.9, 119.4, 110.8, 46.0, 21.4. LC-MS (m/z) [M + H]$^+$ calcd for C$_{21}$H$_{17}$ClN$_3$O$_2$ 378.1004, found 378.0929.

1-(4-Chlorobenzyl)-6-methyl-2-(4-nitrophenyl)-1H-benzimidazole **(4j)**: yellow solid, mp 178–180 °C. IR (ν, cm^{-1}): 1601 (C=N), 1518 (C=C), 1342 (N=O). ^{1}H NMR (500 MHz, DMSO-d$_6$, δ ppm): 8.35 (2H, d, J = 8.5 Hz, H$_{Ar}$), 8.00 (2H, d, J = 8.0 Hz, H$_{Ar}$), 7.66 (1H, d, J = 8.0 Hz, H$_{Ar}$), 7.57 (1H, s, H$_{Ar}$), 7.34 (2H, t, J = 8.0 Hz, H$_{Ar}$), 7.14 (1H, d, J = 8.0 Hz, H$_{Ar}$), 6.99 (2H, d, J = 8.0 Hz, H$_{Ar}$), 5.63 (2H, s, –CH$_2$–), 2.44 (3H, s, –CH$_3$). ^{13}C NMR (125 MHz, DMSO-d$_6$, δ ppm): 150.9, 147.9, 143.0, 140.8, 136.4, 134.3, 133.3, 132.2, 130.3, 128.9, 128.1, 125.1, 124.5, 119.4, 110.9, 46.9, 21.5. LC-MS (m/z) [M + H]$^+$ calcd for C$_{21}$H$_{17}$ClN$_3$O$_2$ 378.1004, found 378.0932.

1-Benzyl-2-(furan-2-yl)-6-methyl-1H-benzimidazole **(4k)**: brown solid, mp 140–142 °C. IR (ν, cm^{-1}): 1515 (C=N), 1495 (C=C). ^{1}H NMR (500 MHz, DMSO-d$_6$, δ ppm): 7.92 (1H, d, J = 5.0 Hz, H$_{Ar}$), 7.57 (1H, d, J = 8.5 Hz, H$_{Ar}$), 7.39 (1H, s, H$_{Ar}$), 7.31–7.23 (3H, m, H$_{Ar}$), 7.12–7.07 (4H, m, H$_{Ar}$), 6.71 (1H, dd, J = 4.0, 1.5 Hz, H$_{Ar}$), 5.77 (2H, s, –CH$_2$–), 2.42 (3H, s, –CH$_3$). ^{13}C NMR (125 MHz, DMSO-d$_6$, δ ppm): 145.3, 144.1, 143.4, 137.7, 136.3, 134.3, 133.0, 132.1, 129.2, 127.9, 126.7, 124.9, 119.2, 112.8, 110.8, 47.8, 21.9. LC-MS (m/z) [M + H]$^+$ calcd for C$_{19}$H$_{17}$N$_2$O 289.1335, found 289.1230.

4.3. *In vitro* antibacterial and antifungal activities

The minimum inhibitory concentration (MIC) was determined by the microtitre broth dilution method with positive controls (ciprofloxacin for antibacterial activity and fluconazole for

antifungal activity).[4,29] All bacterial strains were maintained at ± 37 °C for 24–48 h on a nutrient agar medium. Meanwhile, all fungal strains were maintained at ± 25 °C for 48 h on potato dextrose agar. The different concentration gradients (2, 4, 8, 16, 32, 64, 128, 256, 512, and 1024 $\mu g\ mL^{-1}$) of tested compounds and positive controls were prepared in the media. The inoculum was prepared by dilution in broth media of each bacteria and fungi to give a final concentration of $5 \times 10^5\ CFU\ mL^{-1}$. The trays were covered and placed in plastic bags to prevent evaporation and are then incubated at 35 °C for 18–20 h with the bacteria, and at 25 °C for 72 h with fungi. The MIC was determined to be the lowest concentration that completely inhibits the growth of the organism. All MIC determinations were done in triplicates in independent experiments.

4.4. *In vitro* anticancer activity

The cytotoxic activity of the synthesized compounds was evaluated using the methyl thiazolyl tetrazolium (MTT) method. Paclitaxel as anticancer drug was used as the positive control. The MTT assay detects the reduction of yellow tetrazolium by metabolically active cells to be purple formazan measured using spectrophotometry.[2,50] The cells lines were seeded into 96-well plates at a density of 5×10^3 cells per well and replenished with growth media including Eagle's Minimum Essential Medium (EMEM), 10% Fetal Calf Serum (FCS), 2 mM L-glutamine, 100 IU per mL penicillin, and 100 μg per mL streptomycin. The cells were incubated at 37 °C for 24 h in 5% CO_2. A series of concentrations (0.5, 1, 5, 10, 25, 50, 80, and 100 μM) of the tested compounds and paclitaxel in DMSO was then added to each well of the 96-well plate and incubated for 48 h using the control DMSO at the same concentration. Next, the plate was incubated at 37 °C for 4 h in a CO_2 incubator after 10 μL fresh solution of MTT reagent was added to each well. Finally, after the purple precipitate was obtained, the cells were dissolved in ethanol and their optical density was recorded at 570 nm using a microplate reader. The experiment was conducted on 6 wells for each concentration of the test sample. The percent of proliferation inhibition was calculated using the following formula:

$$\text{Viability cell inhibition } (\%) = 100 - \left[\frac{(\text{OD}_t - \text{OD}_b)}{(\text{OD}_c - \text{OD}_b)}\right] \times 100\%$$

where OD_t is the optical density of test compound, OD_b is the optical density of blank, OD_c is the optical density of control.

The 50% inhibitory concentration (IC_{50}) of each compound was calculated using the correlation plot between percent of proliferation inhibition and corresponding concentration *via* Graphpad Prism version 8.30.

4.5. ADMET predictions

The physicochemical properties of all compounds were calculated using the SwissADME web tool and ADMETlab 2.0 descriptors algorithm protocol. *In silico* prediction of the ADME (absorption, distribution, metabolism, and excretion) properties and the toxicity (T) risks was performed using ADMETlab 2.0 descriptors algorithm protocol.[49]

4.6. *In silico* molecular docking studies

The structure of ligands were drawn in ChemBioDraw Ultra 19. The energy of these ligands was minimized using ChemBio3D Ultra 19. Protein molecules of dihydrofolate reductase (PDB ID: 4HOF and 3FYV), *N*-myristoyl transferase (PDB ID: 1IYL), gyrase B (PDB ID: 4URM), vascular endothelial growth factor receptor 2 (PDB ID: 5EW3), fibroblast growth factor receptor 1 (PDB ID: 5A46), and histone deacetylase 6 (PDB ID: 5EEF) were retrieved from the protein data bank (https://rcsb.org). After all the water molecules have been removed, the receptors were added to only polar hydrogen and Kollman charges. The grid box for docking simulations was set by AutoDock tools. Next, the ligand molecules with minimized energy were inputted and carried out in the docking simulation using AutoDock Vina.[51]

All the minimizations were performed by AutoDock Vina docking simulation protocol with AMBER force field and the partial charges were automatically calculated. The electrostatic potential was shown for the interaction of two oppositely-charged atoms with a full atomic charge. The search algorithm of AutoDock Vina is a Monte-Carlo iterated search combined with the BFGS17 gradient-based optimizer, which comprises iterations of sampling, scoring, and optimization. AutoDock Vina actually uses a united-atom scoring function (one that involves only the heavy atoms) with combines knowledge-based and empiric scoring function features as well as supports the AutoDock4.2 scoring function.[52] Besides, Auto-Dock Vina was compiled and run under Windows 10.0 Professional operating system. Discovery Studio 2021 was used to deduce the pictorial representation of the interaction between the ligands and the target protein.

4.7. *In vitro* dihydrofolate reductase inhibition assay

The dihydrofolate reductase (DHFR) inhibition assay was performed as per the manual of the CS0340 DHFR assay kit (Sigma, USA). 10 mM stock solutions of dihydrofolic acid and NADPH (reduced nicotinamide adenine dinucleotide phosphate) were prepared in assay buffer with a pH value of 7.5. The five different concentrations (10^{-8}, 10^{-7}, 10^{-6}, 10^{-5}, and 10^{-4} M) of the test compounds and methotrexate (as a positive control) in DMSO solvent were added to the respective wells of the 96-well plate containing assay buffer so the final concentration of DMSO was 0.4% in each experiment. The changes in absorbance were monitored at 340 nm wavelength as a function of time using the test samples. After nullifying the effects (such as NADPH, folate, and solvent), the percentage inhibition of enzymatic activity was calculated. The 50% inhibitory concentration (IC_{50}) of each compound was calculated by plotting a graph between percentage inhibition and the corresponding concentration of the compound using Graphpad Prism version 8.[50]

4.8. Statistical analysis

All values are expressed in mean $\pm$ SEM (Standard Error of Mean). The difference in IC_{50} value between tested compounds and positive control was analyzed by one-way ANOVA (analysis of variance) with Tukey HSD (Tukey's honestly significant

difference) post hoc test using Minitab version 19.0 software. The results were considered statistically significant if the p-value < 0.05. The chart is drawn using Microsoft Excel 2021 software.

Author contributions

Em Canh Pham: conceptualization, methodology, investigation, data curation, supervision, writing-original draft preparation, writing – review & editing. Tuong Vi Thi Le: investigation, software. Huong Ha Hong Ly: investigation. Bich Ngoc Thi Vo: investigation. Long Binh Vong: supervision, investigation. Thao Thanh Vu: investigation. Duy Duc Vo: writing – review & editing. Ngoc Vi Tran Nguyen: investigation. Khanh N. B. Le: supervision, investigation. Tuyen Ngoc Truong: data curation, supervision, writing-original draft preparation, writing – review & editing.

Conflicts of interest

The authors have stated that there is no conflict of interest associated with the publication and no financial support, which could have influenced the outcome.

References

1 B. T. Buu Hue, H. T. Kim Quy, W. K. Oh, V. D. Duy, C. N. Tram Yen, T. T. Kim Cuc, P. C. Em, T. P. Thao, T. T. Loan and M. V. Hieu, *Tetrahedron Lett.*, 2016, **57**, 887–891.

2 P. C. Em, T. N. Tuyen, D. H. Nguyen, V. D. Duy and D. T. Hong Tuoi, *Med. Chem.*, 2022, **18**, 558–573.

3 S. Yadav, B. Narasimhan and H. Kaur, *Anticancer Agents Med. Chem.*, 2016, **16**, 1403–1425.

4 P. C. Em, L. T. Tuong Vi and N. T. Tuyen, *RSC Adv.*, 2022, **12**, 21621–21646.

5 T. H. Kim Chi, T. N. Hong An, T. N. Cam Thu and T. H. Kim Dung, *RSC Adv.*, 2020, **10**, 20543.

6 M. Tunçbilek, T. Kiper and N. Altanlar, *Eur. J. Med. Chem.*, 2009, **44**, 1024–1033.

7 H. Z. Zhang, G. L. Damu, G. X. Cai and C. H. Zhou, *Eur. J. Med. Chem.*, 2013, **64**, 329–344.

8 S. Malasala, M. N. Ahmad, R. Akunuri, M. Shukla, G. Kaul, A. Dasgupta, Y. V. Madhavi, S. Chopra and S. Nanduri, *Eur. J. Med. Chem.*, 2021, **212**, 112996.

9 K. C. Achar, K. M. Hosamani and H. R. Seetharamareddy, *Eur. J. Med. Chem.*, 2010, **45**, 2048–2054.

10 N. Pribut, A. E. Basson, W. A. L. van Otterlo, D. C. Liotta and S. C. Pelly, *ACS Med. Chem. Lett.*, 2019, **10**, 196–202.

11 M. C. Sharma, D. V. Kohli and S. Sharma, *Int. J. Drug Deliv.*, 2010, **2**, 228–237.

12 D. C. Cole, J. L. Gross, T. A. Comery, S. Aschmies, W. D. Hirst, C. Kelley, J. I. Kim, K. Kubek, X. Ning, B. J. Platt, A. J. Robichaud, W. R. Solvibile, J. R. Stock, G. Tawa, M. J. Williams and J. W. Ellingboe, *Bioorg. Med. Chem. Lett.*, 2010, **20**, 1237–1240.

13 G. Surineni, Y. Gao, M. Hussain, Z. Liu, Z. Lu, C. Chhotaray, M. M. Islam, H. M. A. Hameed and T. Zhang, *Medchemcomm*, 2019, **10**, 49–60.

14 D. S. Rudra, U. Pal, N. Chowdhury, N. C. Maiti, A. Bagchi and S. Swarnakar, *Free Radic. Biol. Med.*, 2022, **181**, 221–234.

15 M. Gaba, S. Singh and C. Mohan, *Eur. J. Med. Chem.*, 2014, **76**, 494–505.

16 M. Ouattara, D. Sissouma, M. W. Koné, H. E. Menan, S. A. Touré and L. Ouattara, *Trop. J. Pharm. Res.*, 2011, **10**, 767–775.

17 D. Valdez-Padilla, S. Rodriguez-Morales, A. Hernandez-Campos, F. Hernandez-Luis, L. Yepez-Mulia, A. Tapia-Contreras and R. Castillo, *Bioorg. Med. Chem.*, 2009, **17**, 1724–1730.

18 N. Bharti, M. T. Shailendra, G. Garza, D. E. Cruz-Vega, J. Catro-Garza, K. Saleem, F. Naqvi, M. R. Maurya and A. Azam, *Bioorg. Med. Chem. Lett.*, 2002, **12**, 869–871.

19 B. Bhrigu, N. Siddiqui, D. Pathak, M. S. Alam, R. Ali and B. Azad, *Acta Pol. Pharm. Drug Res.*, 2012, **69**, 53–62.

20 A. A. Farahat, M. A. Ismail, A. Kumar, T. Wenzler, R. Brun, A. Paul, W. D. Wilson and D. W. Boykin, *Eur. J. Med. Chem.*, 2018, **143**, 1590–1596.

21 S. Tahlan, K. Ramasamy, S. M. Lim, S. A. A. Shah, V. Mani and B. Narasimhan, *BMC Chem.*, 2019, **13**, 12.

22 B. G. Tuna, P. B. Atalay, G. Kuku, E. E. Acar, H. K. Kara, M. D. Yilmaz and V. C. Ozalp, *RSC Adv.*, 2019, **9**, 36005–36010.

23 H. Joensuu, J. Y. Blay, A. Comandone, J. Martin-Broto, E. Fumagalli, G. Grignani, X. G. Del Muro, A. Adenis, C. Valverde, A. L. Pousa, O. Bouché, A. Italiano, S. Bauer, C. Barone, C. Weiss, S. Crippa, M. Camozzi, R. Castellana and A. Le Cesne, *Br. J. Cancer*, 2017, **117**, 1278–1285.

24 C. Y. Hsieh, P. W. Ko, Y. J. Chang, M. Kapoor, Y. C. Liang, H. H. Lin, J. C. Horng and M. H. Hsu, *Molecules*, 2019, **24**, 3259.

25 G. Mariappan, R. Hazarika, F. Alam, R. Karki, U. Patangia and S. Nath, *Arab. J. Chem.*, 2015, **8**, 715–719.

26 P. Boggu, E. Venkateswararao, M. Manickam, D. Kwak, Y. Kim and S. H. Jung, *Bioorg. Med. Chem.*, 2016, **24**, 1872–1878.

27 D. R. Gund, A. P. Tripathi and S. D. Vaidya, *Eur. J. Chem.*, 2017, **8**, 149–154.

28 E. M. E. Dokla, N. S. Abutaleb, S. N. Milik, D. Li, K. El-Baz, M. W. Shalaby, R. Al-Karaki, M. Nasr, C. D. Klein, K. A. M. Abouzid and M. N. Seleem, *Eur. J. Med. Chem.*, 2020, **186**, 111850.

29 P. C. Em, L. T. Tuong Vi, T. P. Long, T. N. Huong-Giang, N. B. L. Khanh and N. T. Tuyen, *Arab. J. Chem.*, 2022, **15**, 103682.

30 P. Singla, V. Luxami and K. Paul, *Bioorg. Med. Chem.*, 2015, **23**, 1691–1700.

31 S. B. Nabuurs, M. Wagener and J. de Vlieg, *J. Med. Chem.*, 2007, **50**, 6507–6518.

32 S. M. Rizvi, S. Shakil and M. Haneef, *EXCLI J.*, 2013, **12**, 831–857.

33 N. El-Hachem, B. Haibe-Kains, A. Khalil, F. H. Kobeissy and G. Nemer, *Methods Mol. Biol.*, 2017, **1598**, 391–403.

34 M. Congreve, R. Carr, C. Murray and H. Jhoti, *Drug Discov. Today*, 2003, **8**, 876–877.

35 C. A. Lipinski, *Drug Discov. Today Technol.*, 2004, **1**, 337–341.

36 M. M. Morcoss, E. S. M. N. Abdelhafez, R. A. Ibrahem, H. M. Abdel-Rahman, M. Abdel-Aziz and D. A. Abou El-Ella, *Bioorg. Chem.*, 2020, **101**, 103956.

37 Y. Keng Yoon, M. Ashraf Ali, T. S. Choon, R. Ismail, A. Chee Wei, R. Suresh Kumar, H. Osman and F. Beevi, *BioMed Res. Int.*, 2013, **2013**, 926309.

38 L. Shi, T. T. Wu, Z. Wang, J. Y. Xue and Y. G. Xu, *Bioorg. Med. Chem.*, 2014, **22**, 4735–4744.

39 L. V. Nayak, B. Nagaseshadri, M. V. P. S. Vishnuvardhan and A. Kamal, *Bioorg. Med. Chem. Lett.*, 2016, **26**, 3313–3317.

40 Y. K. Yoon, M. A. Ali, A. C. Wei, A. N. Shirazi, K. Parang and T. S. Choon, *Eur. J. Med. Chem.*, 2014, **83**, 448–454.

41 J. Zhang, D. Yao, Y. Jiang, J. Huang, S. Yang and J. Wang, *Bioorg. Chem.*, 2017, **72**, 168–181.

42 N. S. Goud, S. M. Ghouse, J. Vishnu, D. Komal, V. Talla, R. Alvala, J. Pranay, J. Kumar, I. A. Qureshi and M. Alvala, *Bioorg. Chem.*, 2019, **89**, 103016.

43 S. A. Al-Trawneh, J. A. Zahra, M. R. Kamal, M. M. El-Abadelah, F. Zani, M. Incerti, A. Cavazzoni, R. R. Alfieri, P. G. Petronini and P. Vicini, *Bioorg. Med. Chem.*, 2010, **18**, 5873–5884.

44 M. A. Divakar, S. Shanmugam, T. Muneeswaran and M. Ramakritinan, *ChemistrySelect*, 2016, **1**, 6151–6155.

45 X. Deng and M. Song, *J. Enzyme Inhib. Med. Chem.*, 2020, **35**, 354–364.

46 K. Gholivand, M. H. H. Koupaei, F. Mohammadpanah, R. Roohzadeh, N. Fallah, M. Pooyan, M. Satari and F. Pirastehfar, *J. Mol. Struct.*, 2022, **1263**, 133024.

47 Z. Tatiana and S. Alexis, *Infectious Diseases in Cancer Patients: An Overview*, Springer International Publishing, Switzerland, 2015, pp. 295–311.

48 T. Lam, M. T. Hilgers, M. L. Cunningham, B. P. Kwan, K. J. Nelson, V. Brown-Driver, V. Ong, M. Trzoss, G. Hough, K. J. Shaw and J. Finn, *J. Med. Chem.*, 2014, **57**, 651–668.

49 G. Xiong, Z. Wu, J. Yi, L. Fu, Z. Yang, C. Hsieh, M. Yin, X. Zeng, C. Wu, A. Lu, X. Chen, T. Hou and D. Cao, *Nucleic Acids Res.*, 2021, **49**, W5–W14.

50 P. C. Em and N. T. Tuyen, *ACS Omega*, 2022, **7**, 33614–33628.

51 P. C. Em, V. V. Lenh, V. N. Cuong, N. D. Ngoc Thoi, L. T. Tuong Vi and N. T. Tuyen, *Biomed. Pharmacother.*, 2022, **146**, 112611.

52 T. Gaillard, *J. Chem. Inf. Model.*, 2018, **58**, 1697–1706.